2023-05-01

Characterizing Spatial Variability In Soil Co2 Fluxes In The Chihuahuan Desert Using Geostatistical Techniques

Viridiana Orona
University of Texas at El Paso

CHARACTERIZING SPATIAL VARIABILITY IN SOIL CO_2 FLUXES IN THE

CHIHUAHUAN DESERT USING GEOSTATISTICAL TECHNIQUES

VIRIDIANA ORONA

Master's Program in Environmental Science

APPROVED:

Anthony Darrouzet-Nardi, Ph.D., Chair

Lixin Jin, Ph.D.

Marguerite E. Mauritz-Tozer, Ph.D.

Stephen L. Crites, Jr., Ph.D.
Dean of the Graduate School

DEDICATION

I would like to dedicate this to my mom, Rossana Sotres, to my sisters Rossana and Mariana, and to my dad Carlos Orona, knowing that he would have been very proud of me.

CHARACTERIZING SPATIAL VARIABILITY IN SOIL CO_2 FLUXES IN THE CHIHUAHUAN DESERT USING GEOSTATISTICAL TECHNIQUES

by

VIRIDIANA ORONA, B.S.

THESIS

Presented to the Faculty of the Graduate School of

The University of Texas at El Paso

in Partial Fulfillment

of the Requirements

for the Degree of

MASTER OF SCIENCE

Department of Earth, Environmental and Resource Sciences

THE UNIVERSITY OF TEXAS AT EL PASO

May 2023

ACKNOWLEDGEMENTS

I would like to thank everyone who has supported me throughout this journey and has helped me get to where I am: Anthony Darrouzet-Nardi, Lixin Jin, Marguerite Marutiz-Tozer, Diane Doser, Sue Parsons, Briana Salcido, Kalpana Kukreja, Abiodun Ayo-Bali, Jane Martinez, Cat Cort, Lindsey Dacey, Talveer Singh, Elizabeth Hernandez, Kristina Sasser, Kevin Saldaña, and my family. I will be forever grateful for their endless support and guidance. For pushing me and always believing in me even when I couldn’t. I would also like to thank the Ivey family and Jornada LTER for allowing me to conduct research at their property. Financial support for this study is from the National Science Foundation, under award #1853680 and award #2012475.

ABSTRACT

Spatial variability in soil CO_2 efflux across landscapes is an important feature of the 'Critical Zone' within dryland ecosystems. In dryland critical zones, resources are often distributed in patches or resource islands. Although this is particularly true in natural settings, the significance of spatial variability in CO_2 efflux and its patterns also extends to dryland agriculture. In both irrigated and unirrigated systems, human management practices can significantly impact both organic and inorganic carbon cycling processes, highlighting the importance of studying CO_2 efflux in these systems. We examined the spatial patterns of soil CO_2 efflux and quantified the magnitude and scale of spatial autocorrelation using geostatistical techniques in a flood-irrigated pecan orchard and a creosote bush shrubland. Moreover, we explored some of the associated factors that may drive spatial variability in soil CO_2 efflux. Our results indicated that while CO_2 efflux was autocorrelated at short distances, it was quite variable and difficult to predict at larger scales across the study sites. Furthermore, the level of spatial autocorrelation varied depending on water availability, with weaker patterns at intermediate water levels at the flood-irrigated site. We also found that CO_2 efflux had shorter ranges of autocorrelation compared to tree diameter and electrical conductivity. Tree diameter, proximity to the nearest tree and electrical conductivity did show some association with soil CO_2 efflux, but the correlations were weak. Overall, this research provides evidence that electrical conductivity, tree diameter and proximity to the nearest tree are weak predictors of spatial variability in soil CO_2 efflux and that there are likely other unmeasured factors that control spatial variation in soil CO_2 efflux at these sites.

TABLE OF CONTENTS

LIST OF TABLES

LIST OF FIGURES

INTRODUCTION

The carbon cycle is a major biogeochemical process that occurs within the thin layer of the Earth's surface that extends from the top of the vegetation canopy down to the bedrock, also known as the 'Critical Zone' (Giardino & Houser, 2015). Within the critical zone, soils in particular play a crucial role as they are the second-largest carbon pool in this cycle (Hutyra, 2014). Drylands, which account for nearly half of the world's land area, also contribute significantly to the planet's terrestrial carbon inventory (Prăvălie, 2016; Safriel et al., 2005). However, their role in carbon dynamics is not limited to carbon storage. Drylands can function as either carbon sources or sinks depending on climatic conditions. Wet years typically lead to an increase in plant growth, resulting in higher carbon uptake, whereas dry years can trigger the opposite effect (Ahlström et al., 2015; Biederman et al., 2017; Poulter et al., 2014). To determine whether a system will function as a carbon source or sink, we must understand the component fluxes. One of these component fluxes is soil respiration, which is one of the main processes of carbon loss from dryland soils (Metz et al., 2023; Conant et al., 2000). Soil respiration is often measured as soil CO_2 efflux and is one of the most integrative and important indicators of critical zone function at the soil-atmosphere interface (Darrouzet-Nardi et al., 2023). The two main components of soil respiration are autotrophic root respiration and heterotrophic respiration. Heterotrophic respiration can occur in the rhizosphere or bulk soil and involves the activity of bacteria, fungi, and soil fauna (Hanson et al., 2000). In addition to the component fluxes, moisture events are also critical in stimulating ecosystem functions in drylands, including soil respiration. For example, when analyzing soil CO_2 efflux in the Chihuahuan Desert, the highest rates are observed in late July and August following summer rains. (Parker et al., 1983). This is typical in the Chihuahuan Desert where 53% of the total annual precipitation falls during the monsoon season of July through September (Snyder & Tartowski, 2006).

One interesting feature of the carbon cycle in dryland critical zones is the importance of not only organic carbon but also of inorganic carbon in the form of pedogenic carbonates. This is especially true in irrigated agriculture where inorganic carbon fluxes can be substantial (Ortiz et al., 2022; Sanderman, 2012). Pedogenic carbonate forms when dissolved bicarbonate (HCO_3^-) and calcium (Ca^{2+}) react to produce calcite ($CaCO_3$), carbon dioxide (CO_2) and water (H_2O):

$$CaCO_3(s) + CO_2(g) + H_2O \rightleftharpoons 2\ HCO_3^- + Ca^{2+}$$

Soil inorganic carbon in drylands is less dynamic than the organic pools but the total amount in the soil can be up to 10 times greater than that of soil organic carbon (Tan et al., 2014), and it can be a potential source of CO_2 emitted to the atmosphere (Lal & Kimble, 2000; Tamir et al., 2011) (Figure 1.1), as shown by the CO_2 term in the above equation.

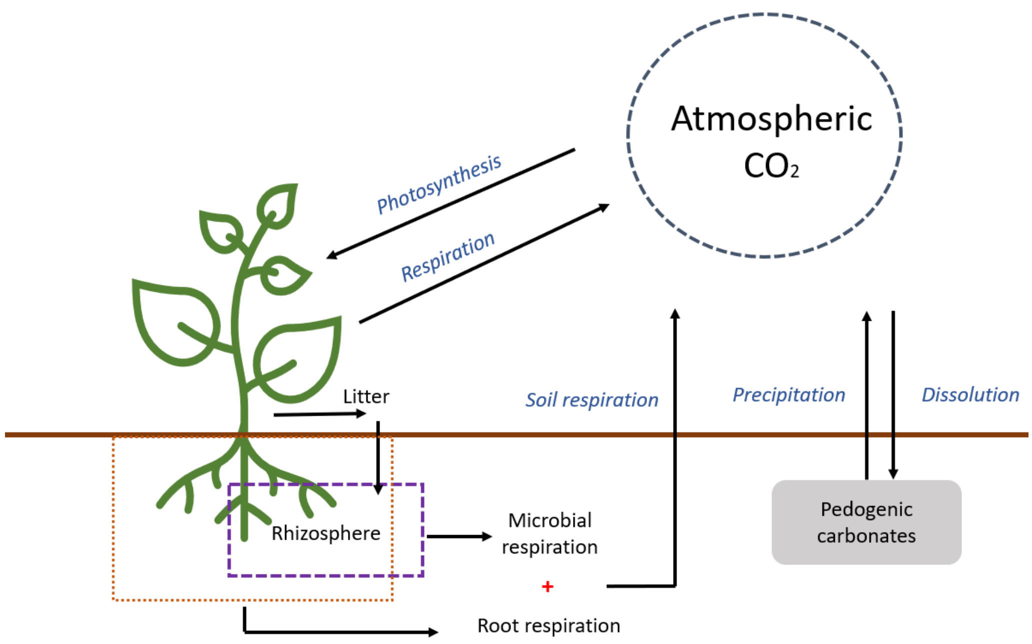

Figure 1.1. CO_2 model diagram of biotic and abiotic factors that contribute to carbon emissions to the atmosphere.

To improve our understanding of these various carbon fluxes, and ultimately carbon balance in drylands, an important factor to consider is spatial variability across dryland landscapes. In semiarid regions where resources are distributed in patches or resource islands, there can be significant spatial variability (Schlesinger & Pilmanis, 1998). These patchy landscapes thus make spatial variation in soil CO_2 efflux an important consideration. Although this is particularly true in natural settings, the significance of spatial variability and its patterns also extends to dryland agriculture. Unlike natural systems, basic farm management practices such as planting crops, adjusting water inputs, adding soil nutrients, and other activities significantly impact both organic and inorganic carbon processes (Entry et al., 2004; Lal & Kimble, 2000; Wu et al., 2009).

One way to quantify and predict the spatial variability of soil CO_2 efflux is through geostatistical techniques such as semivariograms and kriging (Herbst et al., 2012; La Scala et al., 2000; Panosso et al., 2009; Stoyan et al., 2000). Understanding spatial controls of CO_2 dynamics are relevant for improving biophysical process models that estimate CO_2 fluxes in terrestrial ecosystems (Carvalhais et al., 2010; Luo et al., 2008) at different scales such as landscape and regional. While many studies have investigated spatial variation of soil CO_2 efflux in forest ecosystems (Biederman et al., 2017; Buchmann, 2000; Norman et al., 1997; Rayment & Jarvis, 2000), less information exists on arid and semiarid ecosystems (Leon et al., 2014; Maestre & Cortina, 2002). This project will help to define linkages between irrigation, salt build up, and soil-atmospheric CO_2 exchange in desert agricultural and natural soils of the southwestern United States by characterizing spatial patterns in CO_2 efflux.

The aim of this study is to characterize spatial variation and explore some of the controlling factors that drive spatial variability of soil CO_2 at two dryland sites with different land uses: an irrigated pecan orchard, and an unirrigated creosote bush shrubland. Both sites are located in the Chihuahuan Desert. Our aim was to address the following questions: (1) What are the spatial patterns of CO_2 efflux in (a) the creosote shrubland and (b) a flood-irrigated pecan orchard over the course of an irrigation/watering cycle? (2) How spatially autocorrelated are the CO_2 effluxes and how do they compare to other measured critical zone features? and (3) Are proximity to the closest tree or tree size good predictors of CO_2 spatial variation at the flood-irrigated pecan orchard? To address these questions, we conducted spatial surveys to characterize soil CO_2 efflux patterns and measured CO_2 efflux rates using a chamber system with a portable infrared gas analyzer. To complement the spatial surveys, we monitored the diurnal fluctuations in soil CO_2 efflux using a static chamber. We then applied geostatistical techniques to quantify the magnitude and scale of spatial heterogeneity in soil CO_2 fluxes and other subsurface features. Lastly, we examined associations between these spatial patterns with other aspects of the critical zone.

METHODS

2.1 Study Sites

The primary study site for this work was a pecan orchard along the Rio Grande River near Tornillo, Texas in El Paso County (31.404480°, -106.054725°) (Figure 2.1). It is a useful site to perform this study because it's representative of Chihuahuan Desert irrigated agriculture, and it has been the location of ongoing examinations of critical zone processes (Ortiz & Jin, 2021). Climatic conditions in the Chihuahuan Desert are between arid and semiarid, where the mean annual precipitation is ~16-25 cm and the annual potential evapotranspiration is ~194 cm (1981-2010) (Arguez et al., 2012; Ganjegunte et al., 2018). The soils are composed of stratified alluvial sands, loams and clays originated from the ancient Rio Grande river (Longenecker et al.,1963; Ortiz & Jin, 2021). Flood irrigation in the pecan orchard usually occurs every two to three weeks during the growing season (April to October). River water is used for irrigation and groundwater when river water is scarce, averaging at 1.5 m of water per year (Ortiz & Jin, 2021).

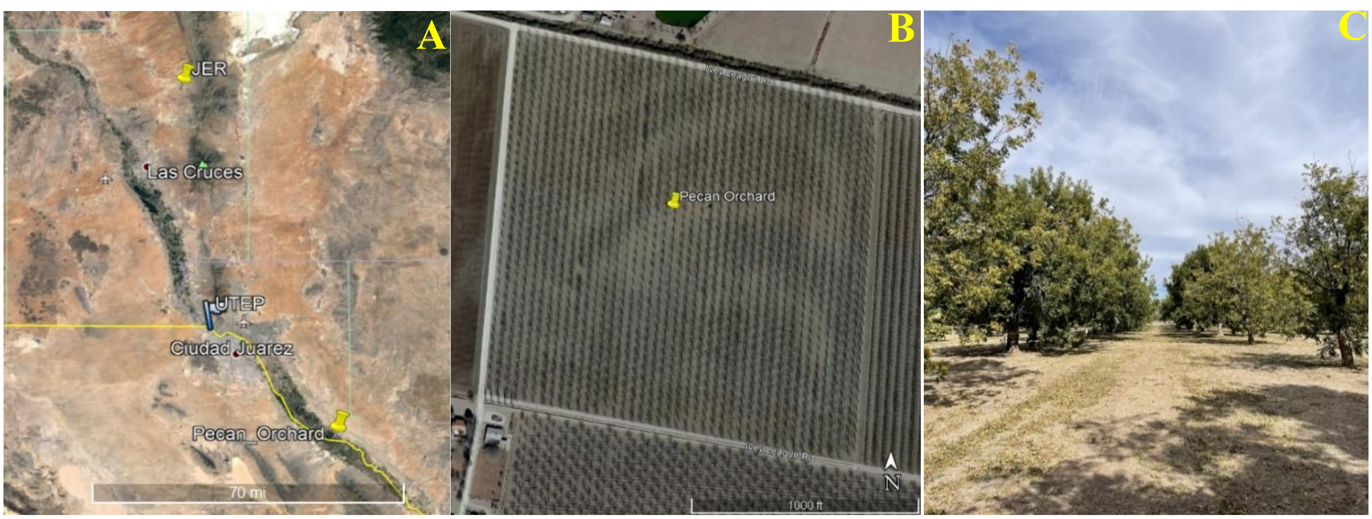

Figure 2.1. Flood-irrigated pecan orchard agricultural managed field site along the Rio Grande River, Tornillo, Texas, USA. (A) is the location area map, (B) pecan orchard aerial photograph, and (C) "street" view of the pecan orchard.

The creosote bush shrubland is located at the Jornada Experimental Range that is located 37 km north of Las Cruces in Dona Ana County, New Mexico (32.581956 N, -106.635025 W) (Figure 2.2), with a mean annual precipitation of 247 mm (Robert P. Gibbens & Lenz, 2001) and a mean monthly maximum temperature that ranges from 13^{o} C in January to 36^{o} C in June (Havstad et al., 2000). The Jornada Experimental Range is located between the Rio Grande floodplain on the east and to the western slopes of the San Andres Mountains. Soils have formed from fluvial materials deposited by the ancestral Rio Grande and washed in from surrounding mountains (Robert P. Gibbens & Lenz, 2001). Vegetation at the Jornada Experimental Range is generally classified as desert grassland (McClaran, 1995) and is currently dominated by the C3 shrubs creosote bush (*Larrea tridentata*) and honey mesquite (*Prosopis glandulosa*) (Bergametti & Gillette, 2010; R. P. Gibbens et al., 2005; Serna-Pérez et al., 2006).

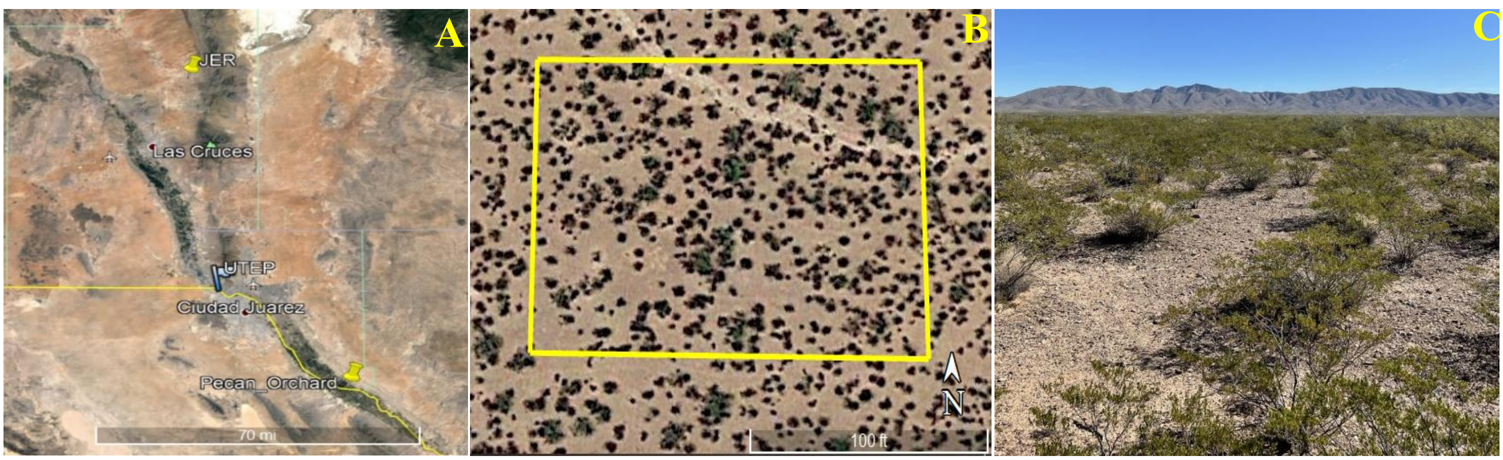

Figure 2.2. Creosote bush shrubland site at Jornada Experimental Range located near Las Cruces in Dona Ana County, New Mexico, USA, (32.581956 N, -106.635025 W). (A) is the location area map, (B) aerial photograph and (C) "street" view.

2.2 Spatiotemporal soil CO_2 efflux from stationary and portable chambers

To characterize patterns of CO_2 spatial variation, a total of seven spatial surveys were conducted at the flood-irrigated pecan orchard before, during, and after the irrigation season between 2021 and 2022 in which soil CO_2 efflux was measured *in situ* using a portable chamber system containing an infrared gas analyzer (EGM-5 with SRC, Environmental Gas Monitor for CO_2, PP Systems, U.S.A). To develop a set of spatial locations for sampling, 80% of the measurement points were placed on a regular hexagonal grid to ensure complete coverage of the site, and 20% were randomly located to fill out smaller distance-pairs on a semivariogram (Darrouzet-Nardi & Bowman, 2011). The total sample area is ~110 × 110 m and points were spaced at distances of ~15 m, with 83 sampling points in total (Figure 2.3).

Measurements of soil CO_2 efflux were taken at each measurement location between 10:00 and 15:00 local time (MST). This time of day was selected for measurements because midday has been shown to be the average peak positive flux for soil CO_2 efflux (carbon loss from the ecosystem to the atmosphere) in a dryland ecosystem (Darrouzet-Nardi et al., 2015). The EGM-5 was placed on the ground surface at the previously located points with the help of a high precision mapping unit (TOPCON GMS-2). This unit integrates the Global Positioning System (GPS) and the Global Navigation Satellite System (GLONASS L1) that helps improve the accuracy of the surveying points. An external PG-A5 antenna was connected to ensure precision at centimeter-level. The sampling period of each point was done as quickly as possible to avoid soil temperature variation in the grid. Only one reading was taken at each point due to the time it takes (1-3 minutes) for the sensor to capture the CO_2 flux rate in the soil, and the small-time frame we had from the average peak positive flux for net respiration.

The spatial surveys were conducted seven times, one on each date of 2021-02-06, 2021-05-14, 2022-08-11, 2022-10-21, 2022-10-29, 2022-11-05 and 2022-11-19. This sequence of dates corresponds to the yearly irrigation pattern, progressing from the driest to the wettest periods. It begins in February, prior to the irrigation season, then moves on to the May and August dates that fall within the irrigation season, and lastly concludes with October and November. The four measurements during October and November are a sequence of measurements that follow a single dry-down event after the last irrigation event of the season (September 17, 2022); thus, sampling dates were closer together compared to those during the previous irrigation events. Measurements were taken during the wet period that followed the late rains, which caused the irrigation scheduled for October to be canceled, and extended the period before the field was accessible for dry-down. The field can take two days to irrigate and at least ten days to dry down before being accessible, but it can vary depending on air temperature and precipitation events.

At the creosote bush shrubland we conducted three spatial surveys for comparison between two land uses: irrigated vs. non-irrigated (Figure 2.3). The surveys were conducted one day before and one day after a water saturation experiment in spring 2021. During this experiment, ~60-90 mm of water were added to a 10 × 20 m irrigated plot. An additional survey was conducted in November 2022. The sampling area was reduced because of the vegetation size being smaller compared to the size of the pecan trees. The measurement locations were spaced at distances of ~5 m with 81 sampling points in a total area of ~40 × 40 m. The same field sampling procedure was followed at both sites.

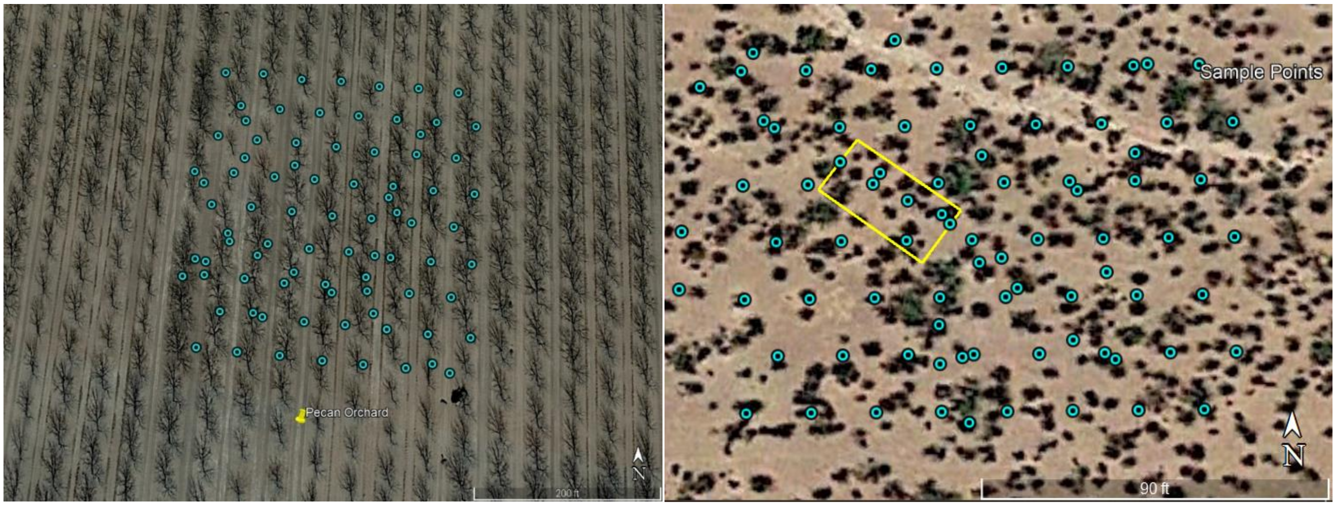

Figure 2.3. Hexagonal grid of sampling points at the flood-irrigated pecan orchard (A) and Jornada Experimental Range the creosote bush shrubland (B). The yellow square represents the saturation experiment plot.

To complement the spatial surveys, we monitored the daily fluctuations in soil CO_2 efflux using a static chamber (eosFD) and compared them with the EGM-5 spatial measurements to examine consistency between the two techniques at both sites. Soils at the pecan orchard are classified as fine and coarse, so one eosFD sensor was installed beneath the coarser soil texture, while another sensor was placed beneath the finer soil texture. The CO_2 efflux values from the spatial measurements at the creosote bush shrubland were time-corrected because of the higher temporal variability. This was done by predicting the CO_2 efflux value at 11:00 a.m. and adding the value to its linear model residuals.

Other subsurface features like electrical conductivity and tree diameter were used to analyze the relationship between these and CO_2 efflux. The electrical conductivity data was collected from an electromagnetics survey conducted in 2013 by using a Geonics EM31-MK2 instrument. It is expected that the range will be larger at the pecan orchard site because plants are considerably larger compared to the shrubs at the Jornada. The tree diameter for each pecan tree was measured on site.

2.3 Statistical Analyses

To assess the level of spatial autocorrelation among the CO_2 data and other subsurface features such as electrical conductivity and tree diameter, I began by fitting semivariogram models. A semivariogram is a geostatistical tool used to model the spatial autocorrelation of a variable of interest across a geographical area (Figure 2.4). It can be used to quantify the degree of similarity between pairs of observations at different distances apart. The semivariogram is plotted as a function of distance and provides insight into the spatial structure of the data. The main components of a semivariogram include the nugget variance, range, and sill variance. The nugget variance refers to the residual variation at points with no distance between them and it can be found at the y-axis intercept. In theory, the value for a lag distance of zero should be zero. However, deviations from zero may occur due to measurement errors and variations on a small scale, and the nugget variance helps to quantify this phenomenon. The range is where stabilization of semivariogram takes place. It is the distance at which points are no longer spatially correlated. The semivariance stabilization value called sill, is the variance at the range. The partial sill is the difference between the total sill variance and the nugget variance, which we report as a percentage (nugget / [nugget + sill]) to represent the magnitude of spatial autocorrelation. These metrics, the partial sill, range, and coefficient of variation of CO_2 efflux (CV%) together can be used to characterize the amount and types of spatial variation and correlation among samples at various distances and have been previously applied to ecological studies (e.g.,Darrouzet-Nardi, 2010; Darrouzet-Nardi & Bowman, 2011; Schlesinger et al., 1996).

After plotting the semivariogram, the data can show a random or a systematic behavior that can be explained by models using mathematical functions such as spherical or Gaussian (Bohling, 2005). The Gaussian model exhibits a parabolic behavior at the start and is more appropriate for a smooth and continuous spatial structure, while the spherical model shows a linear behavior and is suitable for depicting characteristics that exhibit a greater degree of variability over shorter distances. In general, the choice between the Gaussian and spherical models will depend on the data being analyzed and the specific spatial structure that is present. When the variogram appears as a flat, horizontal, or sloping line, fitting a three-parameter model, such as the spherical model with nugget can be challenging, this is because an infinite number of combinations of sill and range (both very large) can fit to a sloping line. In this study, semivariograms were generated to analyze the spatial autocorrelation of soil CO_2 flux measurements, tree size, and electrical conductivity.

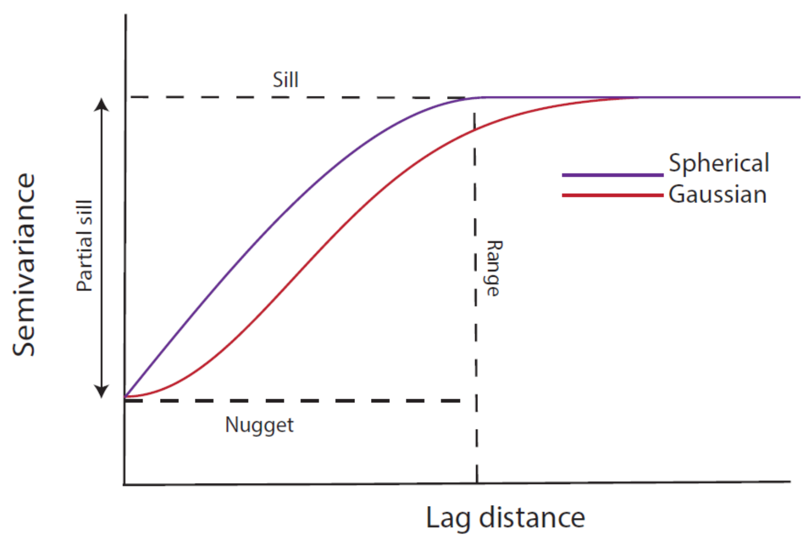

Figure 2.4. Generic semivariogram with spherical and Gaussian models.

Building on the semivariogram models, I also applied another geostatistical technique, kriging, for interpolation of variables across the measurement area. Kriging creates optimal predictions in space based on observations taken at known nearby locations (Cressie, 1990). In this case, a kriged surface based on the electrical conductivity values obtained from the electromagnetics survey, was created to cover the spatial point sampling grid. Later, an electrical conductivity measurement was extracted from each spatial point location in the grid. These measurements were used to calculate linear regressions and coefficient of determination (r^2) to determine the relationship between soil CO_2 efflux and electrical conductivity. Similarly, a kriged surface was created for tree diameter to locate the CO_2 efflux within the big and small trees, but values were not extracted from this analysis because exact diameter measurements of the nearest tree were used. The data were analyzed in ArcGIS (ESRI) to calculate the distance from the spatial CO_2 efflux point to the closest tree m. Linear regressions and the coefficient of determination (r^2) were used to assess the relationship between soil CO_2 efflux vs. tree diameter and vs. the distance to the closest pecan tree. Lastly, a correlation matrix was computed to show the Pearson's correlation coefficient between CO_2 efflux, electrical conductivity, tree diameter and proximity to nearest tree. All analyses were conducted in R 4.2.2 (R Core Team 2021, 2021)

RESULTS

3.1 Spatiotemporal soil CO_2 efflux from stationary and portable chambers

To examine the role of fluctuations in soil CO_2 efflux throughout the day at the flood-irrigated pecan orchard, on which spatial measurements were taken, we compared data from the static chamber that read every 5 minutes (eosFD) with the portable chamber (EGM-5). We monitored the temporal changes in soil CO_2 efflux over the course of the day when the spatial measurements were taken on one day during the irrigation season (Figure 3.1) and one day during the post-irrigation season (Figure 3.2). Temporal measurements were made in the coarse and fine soil in August 2022, and only in the fine soil in November 2022. In August, the mean spatial CO_2 efflux average was 4.68 μmol m^{-2} s^{-1}, while in November, it was 1.33 μmol m^{-2} s^{-1}. The temporal fluxes showed that the fine soil texture had an average of 0.64 μmol m^{-2} s^{-1} in November and 1.73 μmol m^{-2} s^{-1} in August, whereas the coarse soil CO_2 efflux average in August was 2.02 μmol m^{-2} s^{-1}.

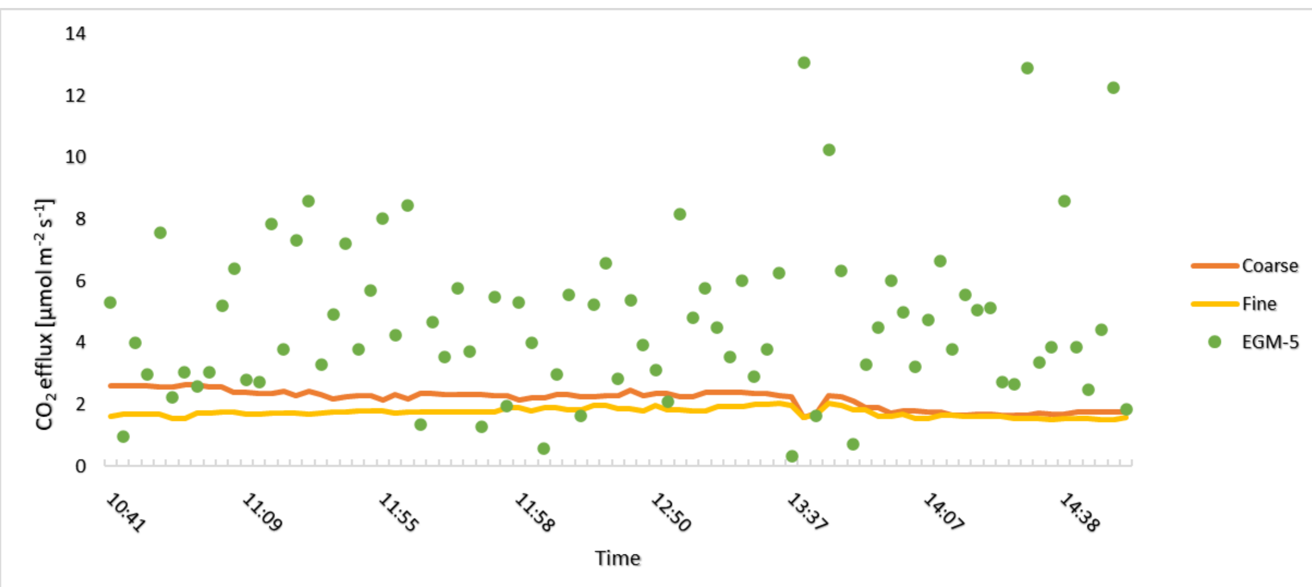

Figure 3.1. Spatial (EGM-5) and temporal (eosFD, coarse and fine soil texture) soil CO_2 efflux measurements for one day during the irrigation season in August 2022 at the pecan orchard.

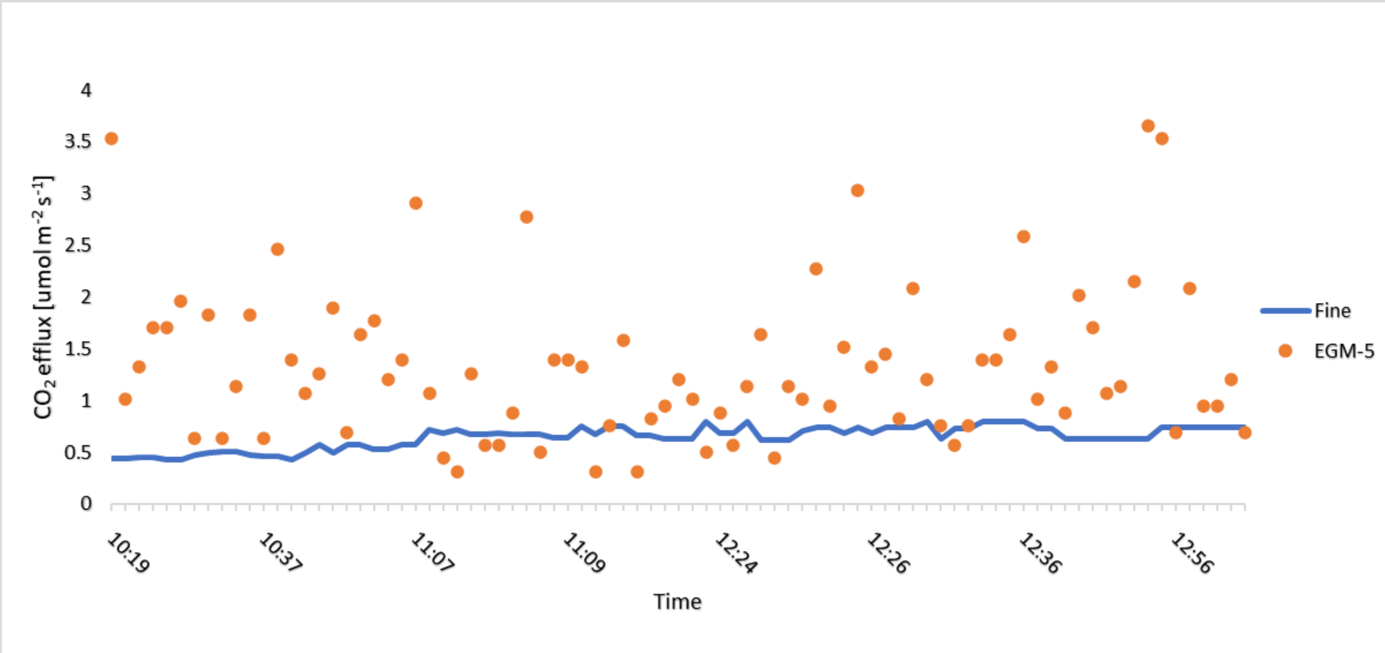

Figure 3.2. Spatial (EGM-5) and temporal (eosFD, fine soil texture) soil CO_2 efflux measurements for one day during the post-irrigation season in November 2022 at the pecan orchard.

To examine the role of fluctuations in soil CO_2 efflux at the creosote shrubland throughout the day on which spatial measurements were taken, we compared data from the static chamber that read every 5 minutes (eosFD) with the portable chamber (EGM-5). We monitored the temporal changes in soil CO_2 efflux over the course of the day when the spatial measurements were taken. We measured CO_2 efflux values before (Figure 3.3) in 2021-03-18 and after a water saturation experiment in 2021-03-20 (Figure 3.4). The mean spatial CO_2 efflux was 0.26 μmol m^{-2} s^{-1} before the saturation experiment and 0.59 μmol m^{-2} s^{-1} after. Mean temporal flux before the saturation experiment was -0.04 μmol m^{-2} s^{-1} and 1.68 μmol m^{-2} s^{-1} after the experiment. It should be noted that some of the spatial measurements were already taken before the eosFD began collecting data in the afternoon.

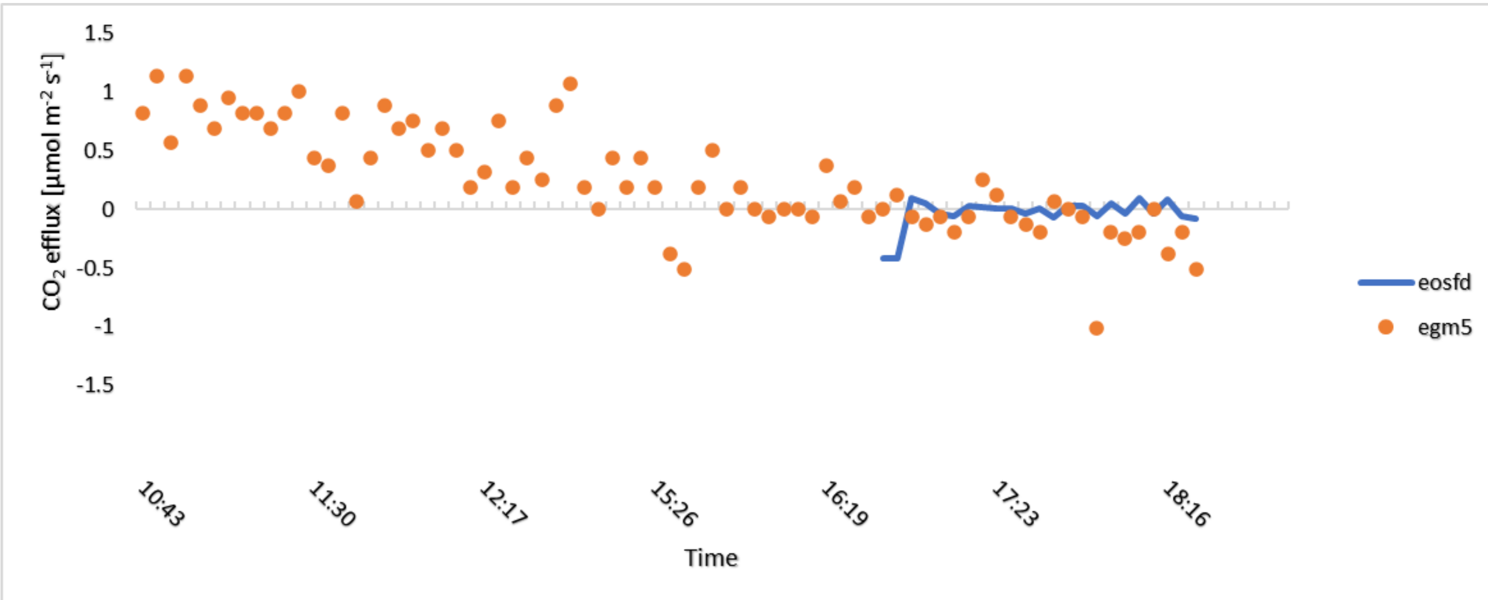

Figure 3.3. Spatial (EGM-5) and temporal (eosFD) soil CO_2 efflux measurements before water saturation experiment on 2021-03-18 at Jornada Experimental Range.

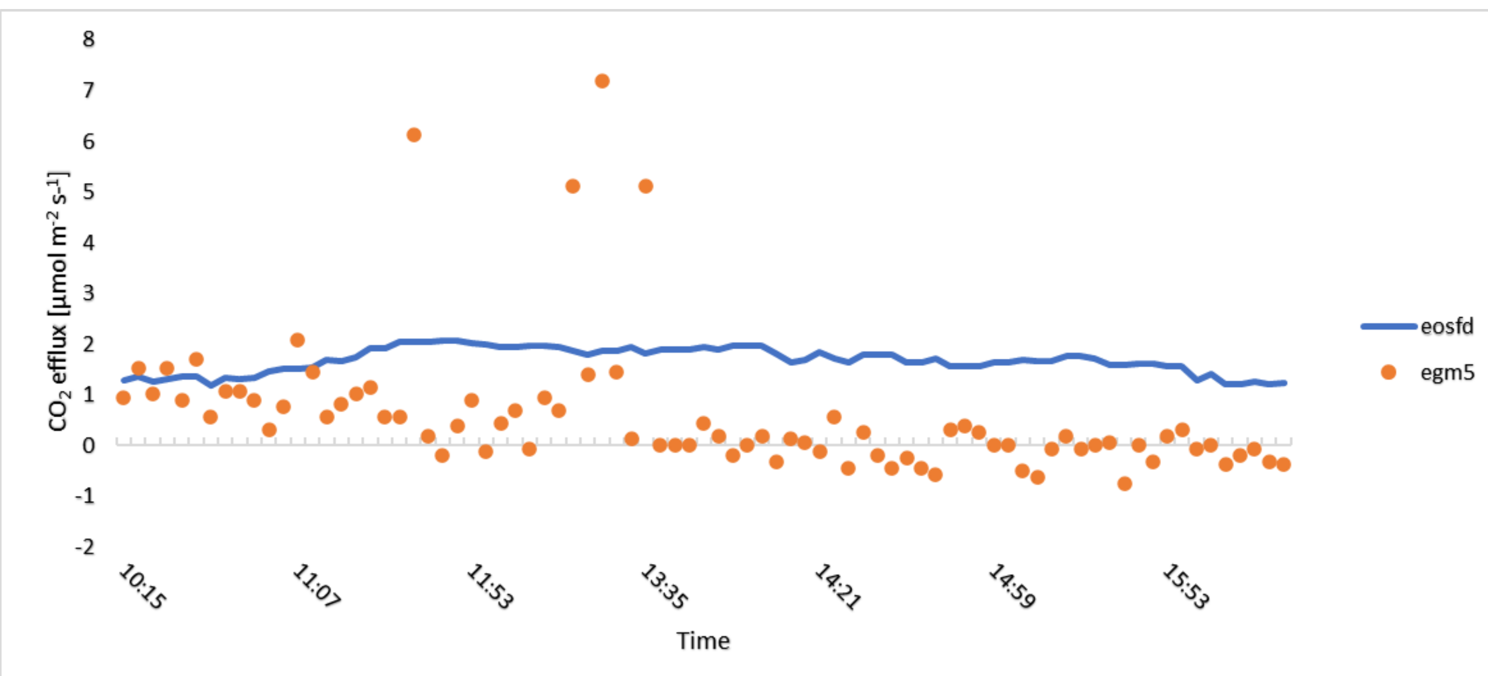

Figure 3.4. Spatial (EGM-5) and temporal (eosFD) soil CO_2 efflux measurements after water saturation experiment on 2021-03-20 at Jornada Experimental Range. Higher values correspond to the irrigated plot from the artificial water experiment.

3.2 Spatial patterns of soil CO_2 efflux

To investigate the spatial patterns of soil CO_2 efflux in the pecan orchard over a flood irrigation cycle, we used the portable chamber (EGM-5) to measure CO_2 efflux rates across a hexagonal grid (Figures 3.5 and 3.6). To complement the current CO_2 efflux data with more details on soil parameters, specific dates indicate the soil temperature (°C) and soil volumetric water content (m^3/m^3) at a depth of 30 cm, limited to fine soil texture based on data availability. Mean values for soil temperature and volumetric water content were calculated for the specific time periods during which the spatial efflux values were measured, which was between 2-4 hours. In February, before the irrigation season, spatial mean efflux values were lowest (0.64 µmol m^{-2} s^{-1}), flux rates increased during the irrigation period in May and in August, with the highest mean values in August (4.68 µmol m^{-2} s^{-1}) and decreased again in October (1.99 and 1.47 µmol m^{-2} s^{-1}) and November (1.34 and 0.84 µmol m^{-2} s^{-1}) during the post-irrigation season. These dates represent the dry down sequence from the last irrigation event on September 17, 2022 (Figure 3.6). Across all sampling dates, CO_2 efflux values ranged from 0.00 to 13.07 µmol m^{-2} s^{-1}, with the highest value recorded in August 2022. The coefficient of variation (CV%) values on each day of sampling ranged from 55.4% – 58.6%, indicating a relatively constant degree of variability between measuring dates, with an outlier in February (90.9%). There was a gradual decrease in mean efflux, mean soil temperature, and mean moisture (VWC) from May through November. Soil moisture was relatively constant at the depth that the sensor was placed (30 cm). Generally, we did not observe obvious spatial CO_2 efflux patterning related to regions within the field. In other words, the CO_2 release is relatively uniform across the field without any significant variations or differences that can be observed visually.

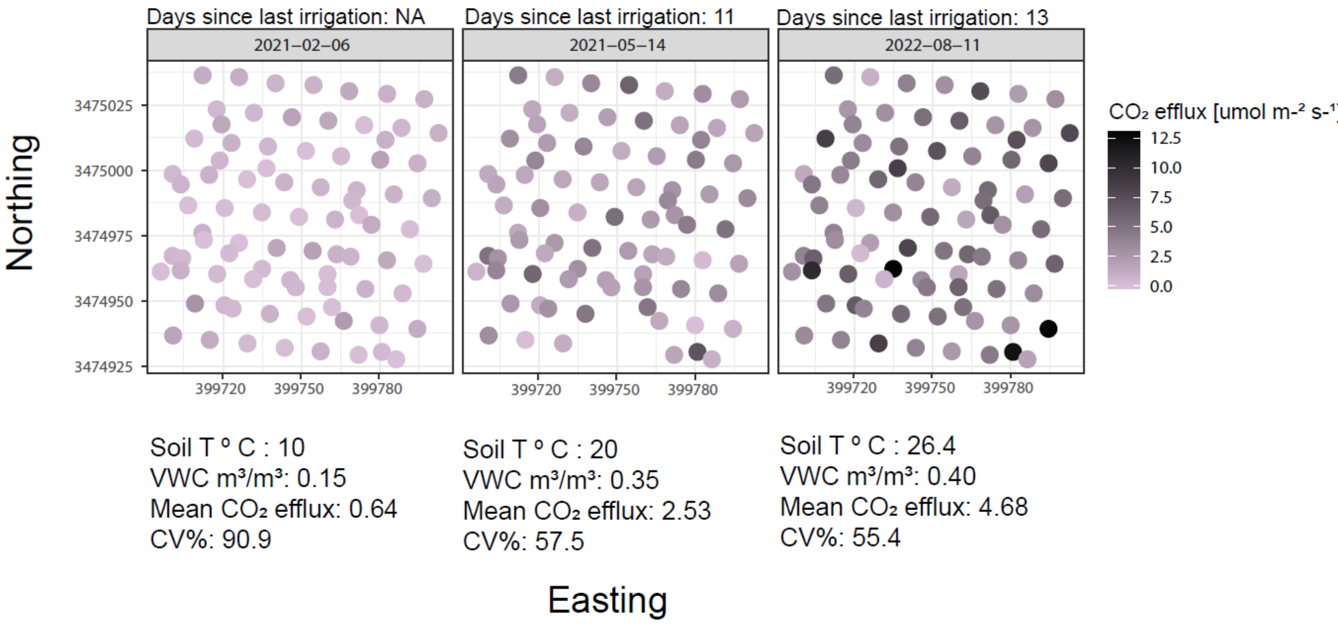

Figure 3.5. Soil CO_2 efflux spatial patterns by date at flood-irrigated pecan orchard during the months of February 2021, May 2021, and August 2022. Mean values of all parameters and coefficient of variation for CO_2 efflux are shown. The volumetric water content (VWC) and soil temperature are 30 cm below surface within fine soil texture.

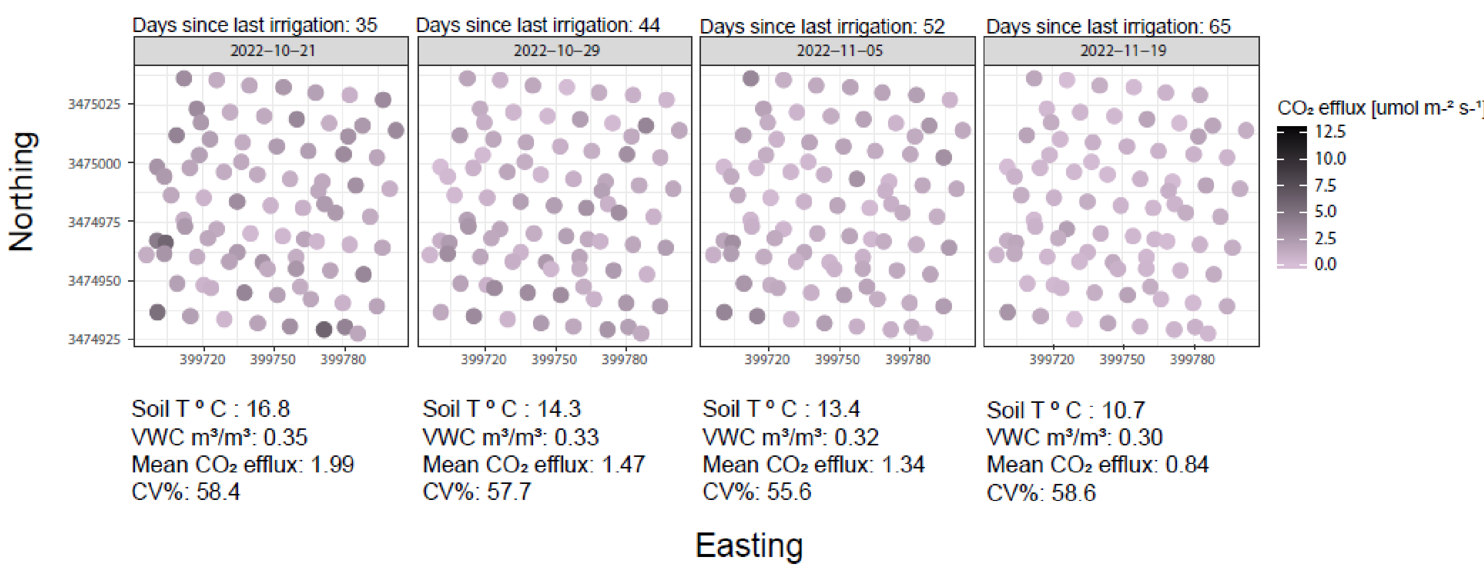

Figure 3.6. Soil CO_2 efflux spatial patterns at flood-irrigated pecan orchard. These dates correspond to the dry down sequence from the last irrigation event on September 17, 2022. Mean values of all parameters and coefficient of variation for CO_2 efflux are shown. The volumetric water content (VWC) and soil temperature are 30 cm below surface within fine soil texture.

To investigate the spatial patterns of soil CO_2 efflux in a creosote shrubland, we used the portable chamber (EGM-5) to measure CO_2 efflux rates across a hexagonal grid (Figure 3.7). The spatial CO_2 efflux pattern displayed in this graph is more uniform during November because the sampling period was shorter, compared to the one on March 18th, that took longer to complete. The pattern before the saturation experiment displays better the daily efflux trend, with higher values in the morning and lower values in the afternoon (Figure 3.7). We observed high CO_2 fluxes on the experimental water saturation plot, after the addition of water on March 20th. When comparing the average CO_2 efflux between sampling dates, we observe that the lowest mean value occurred in 2021-03-18 (0.26 µmol m^{-2} s^{-1}), during spring before the saturation experiment and the highest mean occurred in 2022-11-06 (0.91 µmol m^{-2} s^{-1}). The coefficients of variation (CV) for CO_2 efflux ranged from 40% to 170% on the three dates, with the most variability after the saturation experiment and least variability in November. The variability decreased after the values were corrected to 11:00 for the dates of 2021-03-18, 2021-03-20 and remained relatively constant during 2022-11-06 (Figure 3.8).

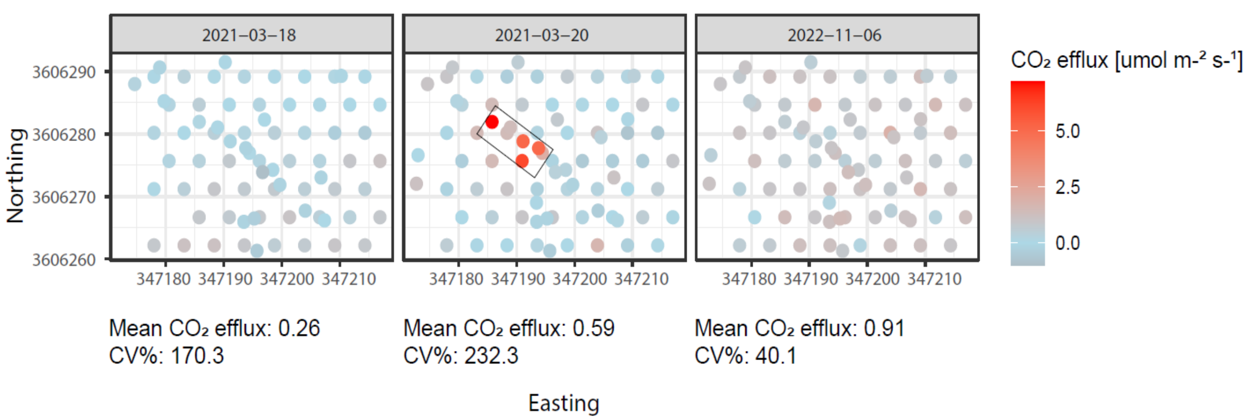

Figure 3.7. Soil CO_2 efflux spatial patterns at Jornada Experimental Range. Higher values correspond to the irrigated plot from the water addition experiment.

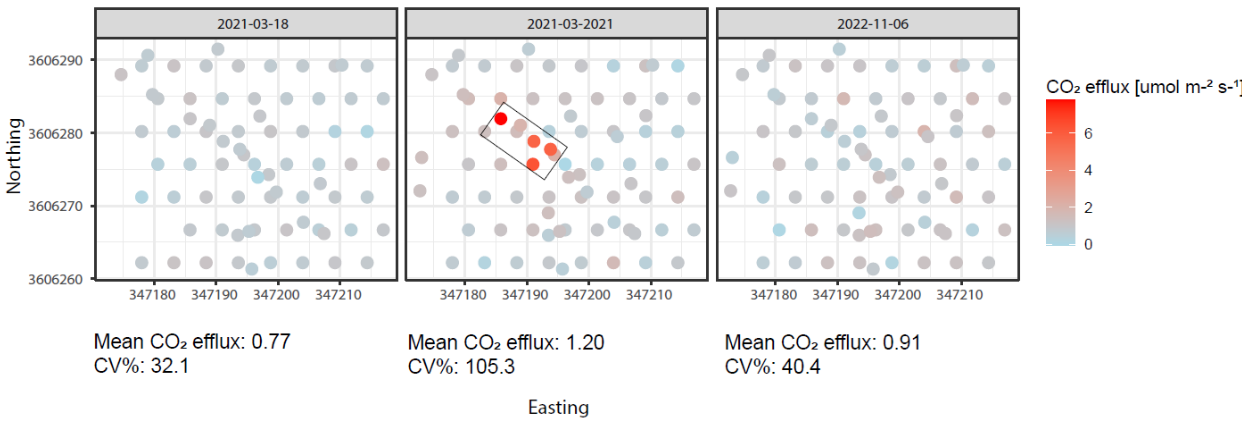

Figure 3.8. Corrected rate values to 11:00 am. Soil CO_2 efflux spatial patterns at Jornada Experimental Range. Higher values correspond to the irrigated plot from the water addition experiment.

3.3 Spatial autocorrelation in soil CO_2 efflux, tree diameter, and proximity to closest tree

Semivariograms were computed to assess the magnitude of spatial autocorrelation of CO_2 efflux, electrical conductivity, and tree diameter at the flood-irrigated pecan orchard (Figure 3.9-3.11). There is a very strong autocorrelation on 2021-05-14, 2022-10-21, 2022-11-05 and 2022-11-19 as indicated by the partial sill (100%), followed by less autocorrelation on 2021-02-06 (88.9%) and least autocorrelation on 2022-08-11 (67.9%). There was no spatial autocorrelation found during 2022-10-29. The scale of spatial autocorrelation decreased in two sampling dates during the irrigation season (2021-05-14 range: 8.5 m and 2022-08-11 range: 5.2 m). Reduced heterogeneity occurred when the field was drier after irrigation season (2021-02-06 range: 15.2 m, and 2022-11-19 range: 15.4 m). The tree diameter had the largest range (74 m). Electrical conductivity was strongly autocorrelated at both depths (98-99%) (Figure 3.10) and the tree diameter was somewhat autocorrelated (66.7%) (Figure 3.11). Tree sizes showed the lowest CV%, followed by the electrical conductivity and then the CO_2 efflux being the highest, with an outlier on 2021-02-06 (Table 1).

Table 1. Descriptive statistics and semivariogram model parameters of the studied properties. SD: standard deviation, CV: coefficient of variation, Psill: partial sill, Range: lag distance, Sph: Spherical, Gau: Gaussian

Date	Mean	SD	CV (%)	Psill (%)	Range m	Model
2021-02-06 (μmol m^{-2} s^{-1})	0.64	0.58	90.9	88.9	15.20	Sph
2021-05-14 (μmol m^{-2} s^{-1})	2.53	1.45	57.5	100.0	8.47	Sph
2022-08-11 (μmol m^{-2} s^{-1})	4.68	2.59	55.4	67.9	5.23	Sph
2022-10-21 (μmol m^{-2} s^{-1})	1.99	1.16	58.4	100.0	8.59	Sph
2022-10-29 (μmol m^{-2} s^{-1})	1.47	0.85	57.7	-	-	-
2022-11-05 (μmol m^{-2} s^{-1})	1.34	0.74	55.6	100.0	14.31	Sph
2022-11-19 (μmol m^{-2} s^{-1})	0.84	0.49	58.6	100.0	15.39	Sph
EC 3m (mS/m)	104.91	37.98	36.2	99.0	27.80	Gau
EC 6m (mS/m)	121.59	39.65	32.6	98.8	24.65	Gau
Tree diameter m	0.41	0.05	12.7	66.7	74.12	Sph

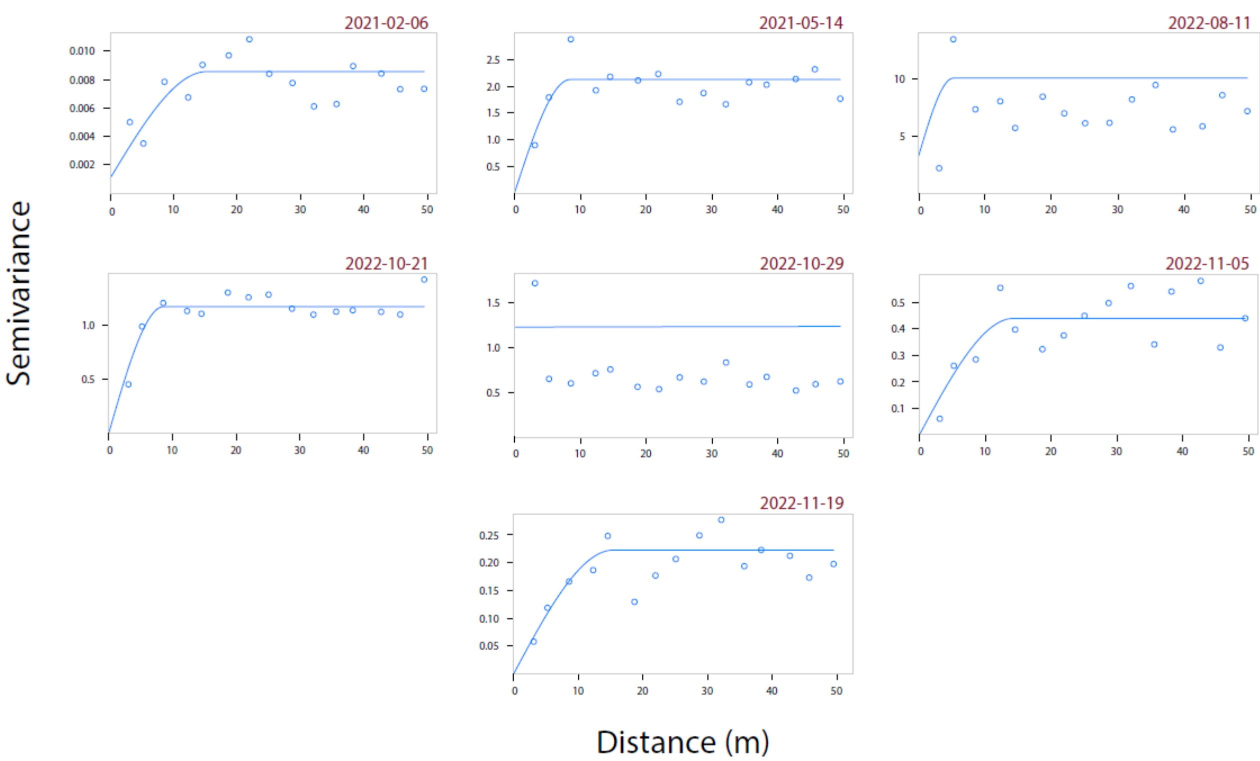

Figure 3.9. Soil CO_2 efflux semivariogram spherical model for all measuring dates. No spatial autocorrelation on 2022-10-29.

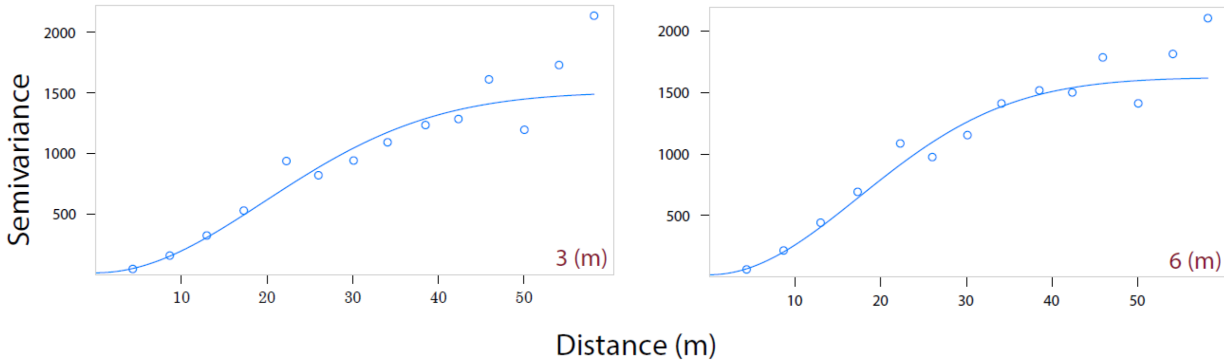

Figure 3.10. Electrical conductivity at 3 m depth (left) and at 6 m depth (right) semivariogram Gaussian model.

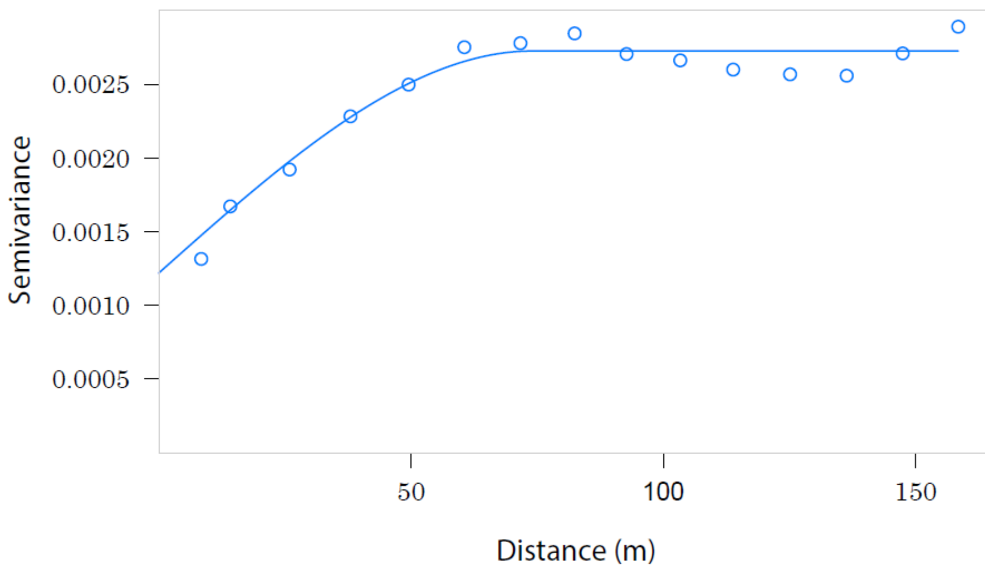

Figure 3.11. Pecan orchard tree diameter m semivariogram spherical model.

3.4 Spatial soil CO_2 efflux autocorrelation at Jornada Experimental Range

Semivariograms were computed to assess the magnitude of spatial autocorrelation of CO_2 efflux at the creosote shrubland (Figure 3.12). There was a very strong spatial autocorrelation on 2021-03-20 after the saturation experiment as indicated by the partial sill (100%), less autocorrelation before the saturation experiment on 2021-03-18 (71.7%) and least autocorrelation on 2022-11-06 (57.1%). The scale of autocorrelation was shorter in 2021-03-18 (range: 1.77 m) before the saturation experiment compared to 2022-11-06 (range: 2.01 m) and increased after the saturation experiment on 2021-03-20 (range 3.49 m). Jornada ranges are smaller compared to the ones at the pecan orchard as predicted, and higher in variability during the saturation experiment sequence (Table 2).

Table 2. Descriptive statistics and semivariogram model for soil CO_2 efflux at Jornada Experimental Range. SD: standard deviation, CV: coefficient of variation, Psill: partial sill, Range: lag distance, Sph: Spherical

Date	Mean	SD	CV (%)	Psill (%)	Range m	Model
2021-03-18 ($\mu mol\ m^{-2}\ s^{-1}$)	0.26	0.44	170.3	71.7	1.77	Sph
2021-03-20 ($\mu mol\ m^{-2}\ s^{-1}$)	0.59	1.37	232.3	100	3.29	Sph
2022-11-06 ($\mu mol\ m^{-2}\ s^{-1}$)	0.91	0.37	40.1	57.1	2.01	Sph

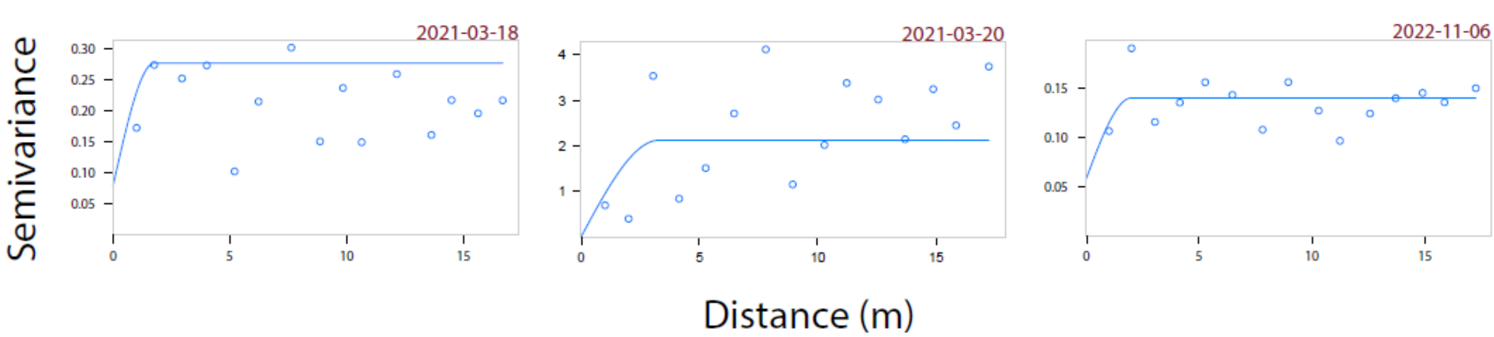

Figure 3.12. Soil CO_2 efflux semivariogram spherical model for all measuring dates at Jornada Experimental Range. No spatial autocorrelation on 2021-18-03.

3.5 Spatial correlates with soil CO_2 efflux

The linear regressions between the electrical conductivity values at 3 m and 6 m depth and spatial CO_2 efflux are shown in Figure 3.14 and 3.16 respectively. A significant positive relationship ($p < 0.05$) was found on the date of 2022-10-21 and a significant negative relationship on 2022-10-29 at 3 m depth. Although there was significance, the relationship is weak $r^2 = 0.04$ and $r^2 = 0.05$ respectively. The linear regressions between the electrical conductivity predicted values at 6 m depth and spatial CO_2 efflux showed a significant positive relationship ($p < 0.05$) on the date of 2022-10-21. This relationship is weak $r^2 = 0.07$, but stronger than at 3 m deep.

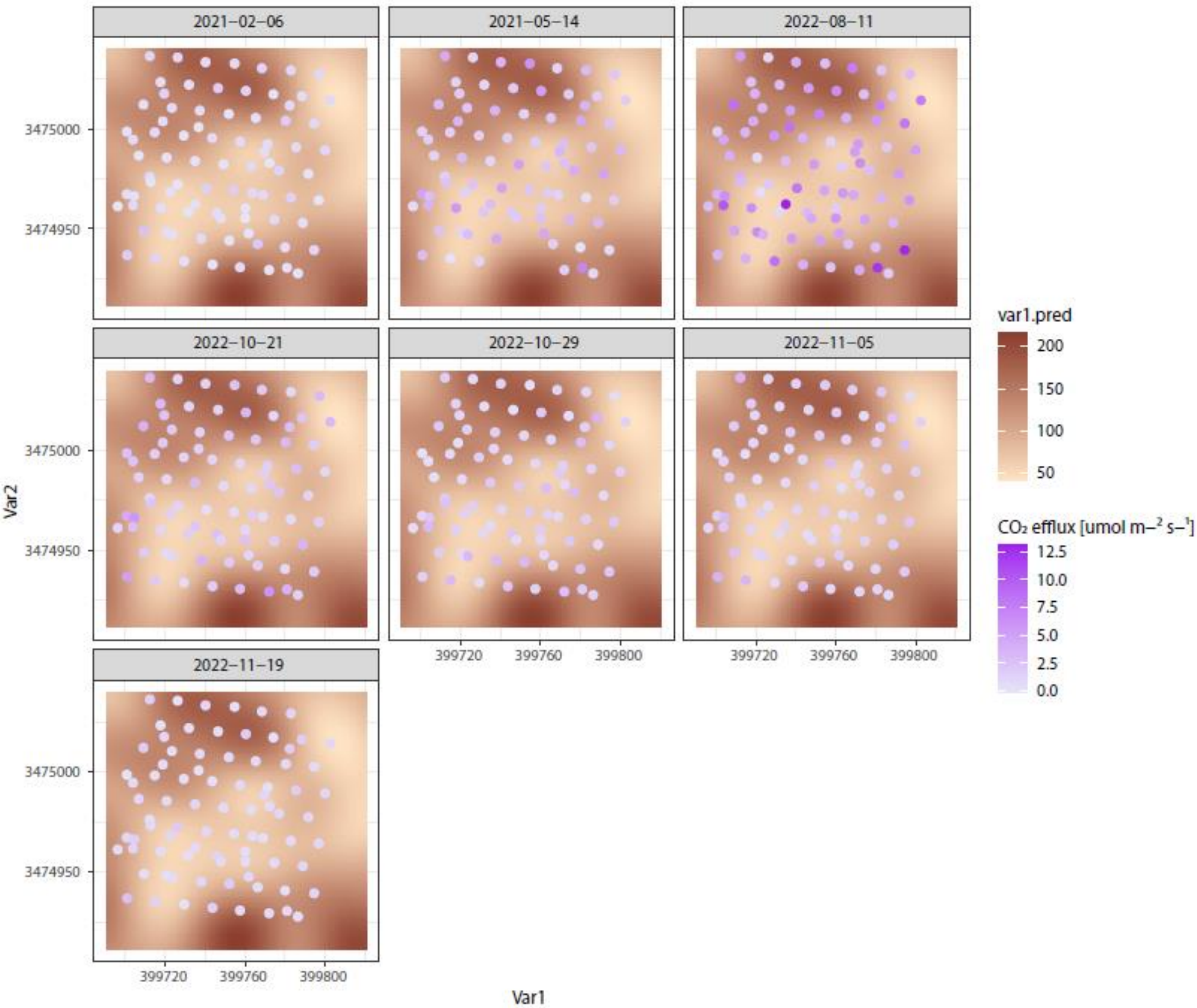

Figure 3.13. Electrical conductivity at 3 m depth kriged surface and spatial CO_2 efflux by date at flood-irrigated pecan orchard.

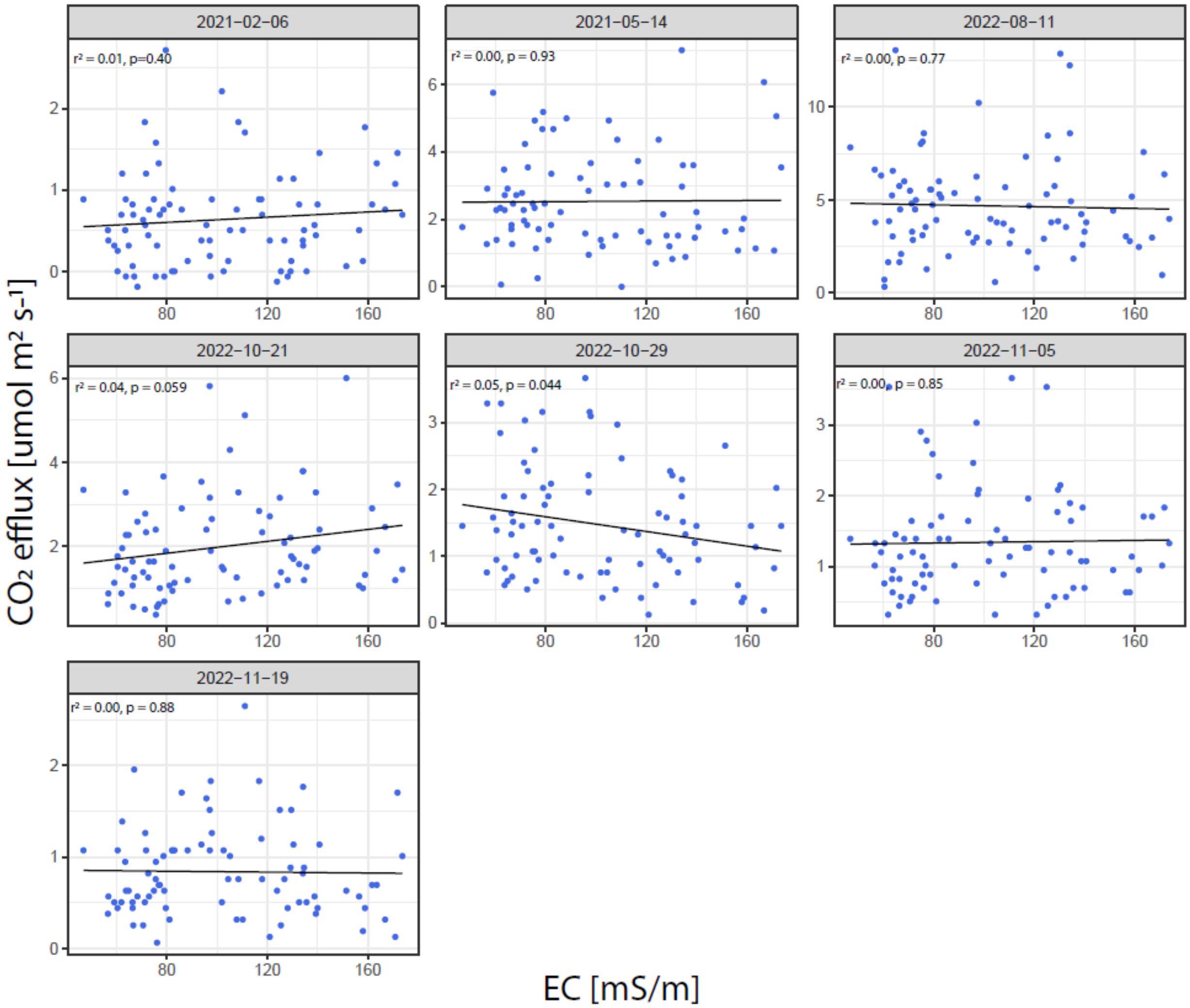

Figure 3.14. Linear regressions by date between electrical conductivity predicted values at 3 m depth and soil CO_2 efflux. Significant ($p < 0.05$) positive relationship on 2022-10-21 $r^2 = 0.04$ and significant negative relationship on 2022-10-29 $r^2 = 0.05$.

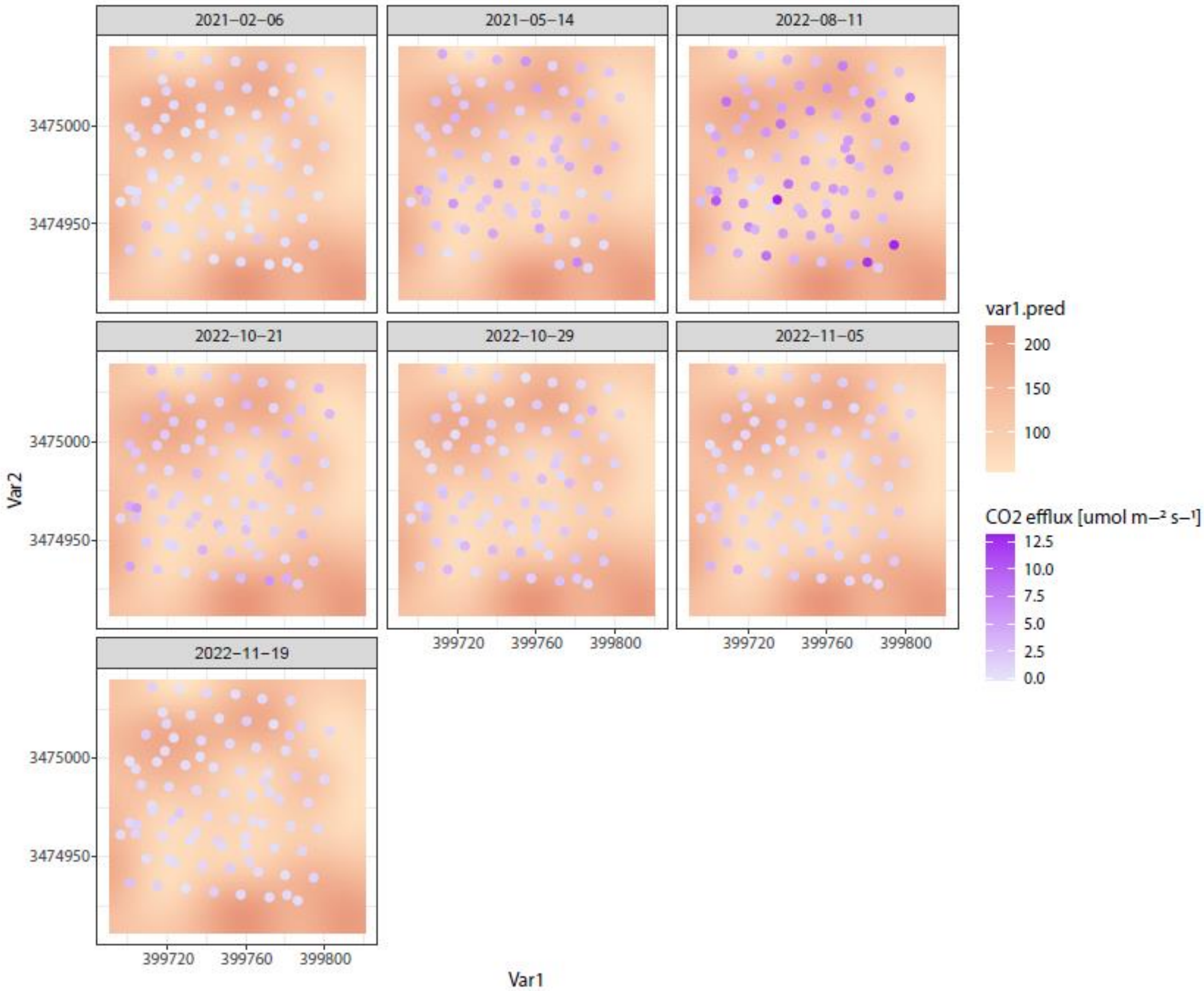

Figure 3.15. Electrical conductivity at 6 m depth kriged surface and spatial CO_2 efflux by date at flood-irrigated pecan orchard.

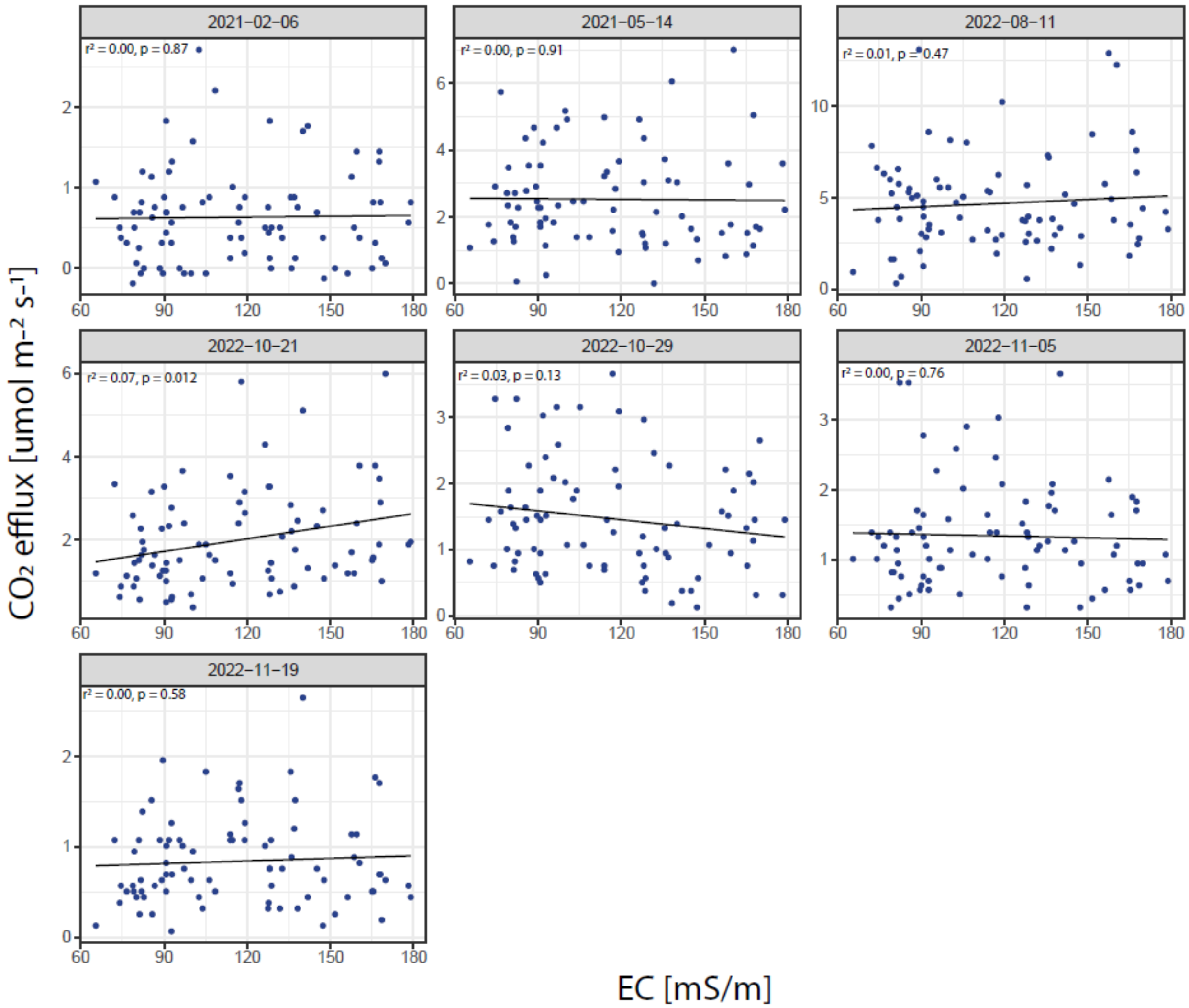

Figure 3.16. Linear regressions by date between electrical conductivity at 6 m depth and soil CO_2 efflux. Significant ($p < 0.05$) positive relationship on 2022-10-21 $r^2 = 0.07$.

The linear regressions between the distance of the CO_2 efflux measurement point and the nearest tree are shown in Figure 3.17. A significant positive relationship ($p < 0.05$) was found on 2022-10-21, 2022-11-05, and 2022-11-19. These are dates that are part of the irrigation dry-down sequence and are 35, 52, and 65 days apart from irrigation, respectively. The regression was weakest on 2022-10-21 $r^2 = 0.05$, slightly stronger on 2022-11-05 $r^2 = 0.11$, and the strongest on 2022-11-19 $r^2 = 0.16$. October and November are post-irrigation months, meaning that as the field dries out from irrigation season, the CO_2 efflux increases farther away from the closest tree. This indicates that CO_2 efflux estimates can be slightly better predicted by measuring the proximity of the CO_2 efflux point to the closest tree for some dates.

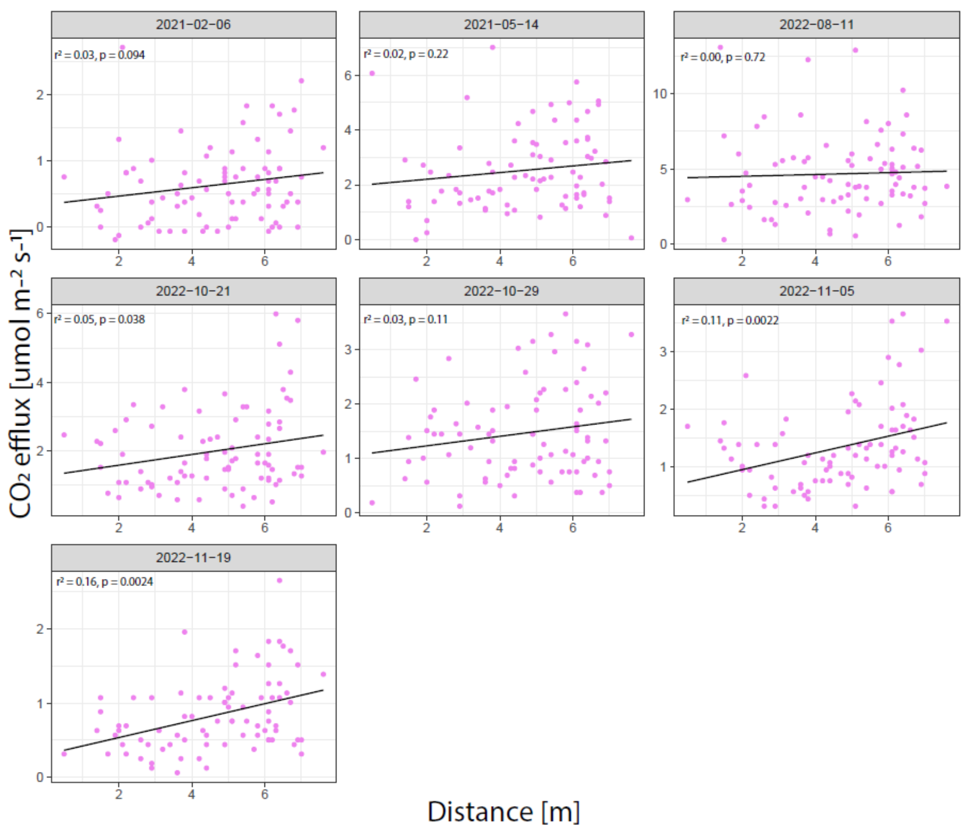

Figure 3.17. Linear regressions by date between distance from CO_2 measuring point to closest tree and soil CO_2 efflux. Significant ($p < 0.05$) positive relationship on 2022-10-21 $r^2 = 0.05$, 2022-11-05 $r^2 = 0.11$, and 2022-11-19 $r^2 = 0.16$.

The linear regressions between CO_2 efflux and nearest tree diameter are shown in Figure 3.19. A significant positive relationship ($p < 0.05$) was found on 2022-11-05 and 2022-11-19, but the correlation is weak $r^2 = 0.04$ and $r^2 = 0.08$. During November, which is a post-irrigation period, larger trees were associated with higher CO_2 fluxes on certain dates as the field dries out from the irrigation season.

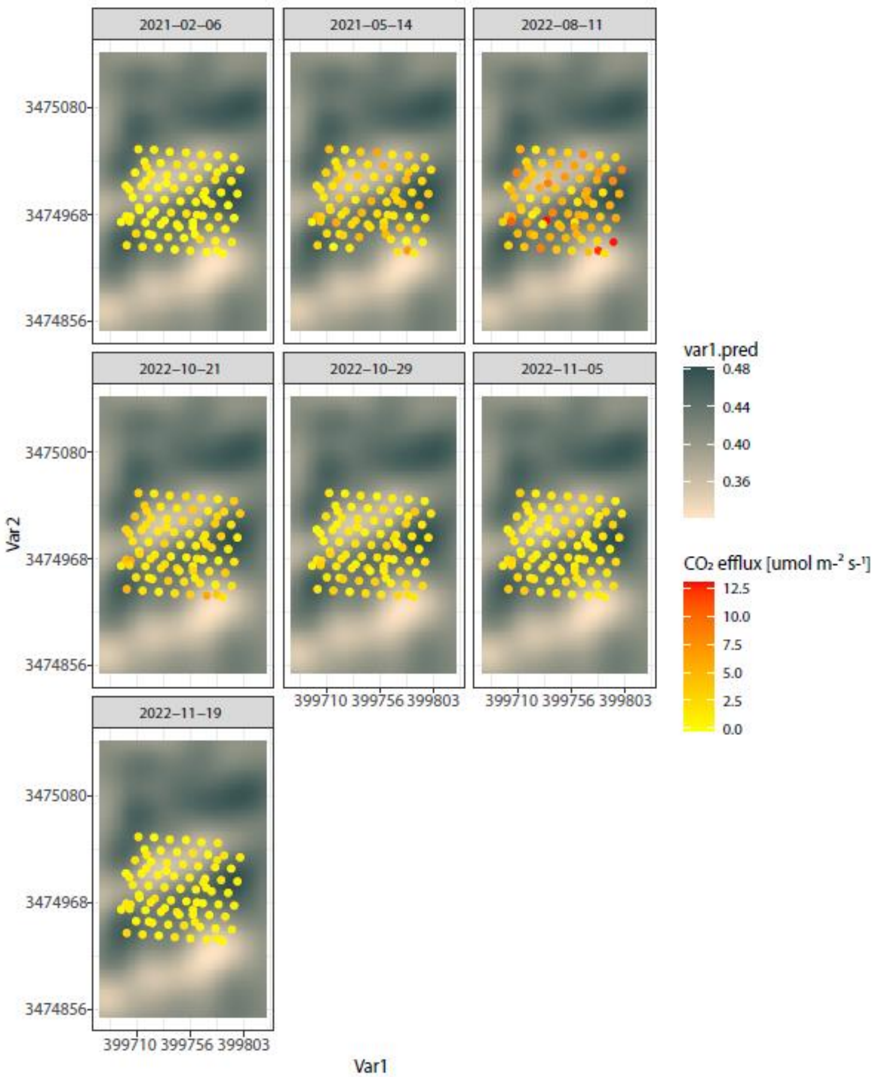

Figure 3.18. Tree size kriged surface and spatial CO_2 efflux by date at flood irrigated-pecan orchard. Bigger trees are dark green and smaller trees in beige. Some of the highest CO_2 efflux values in August are located near the big trees in the dark green shaded area.

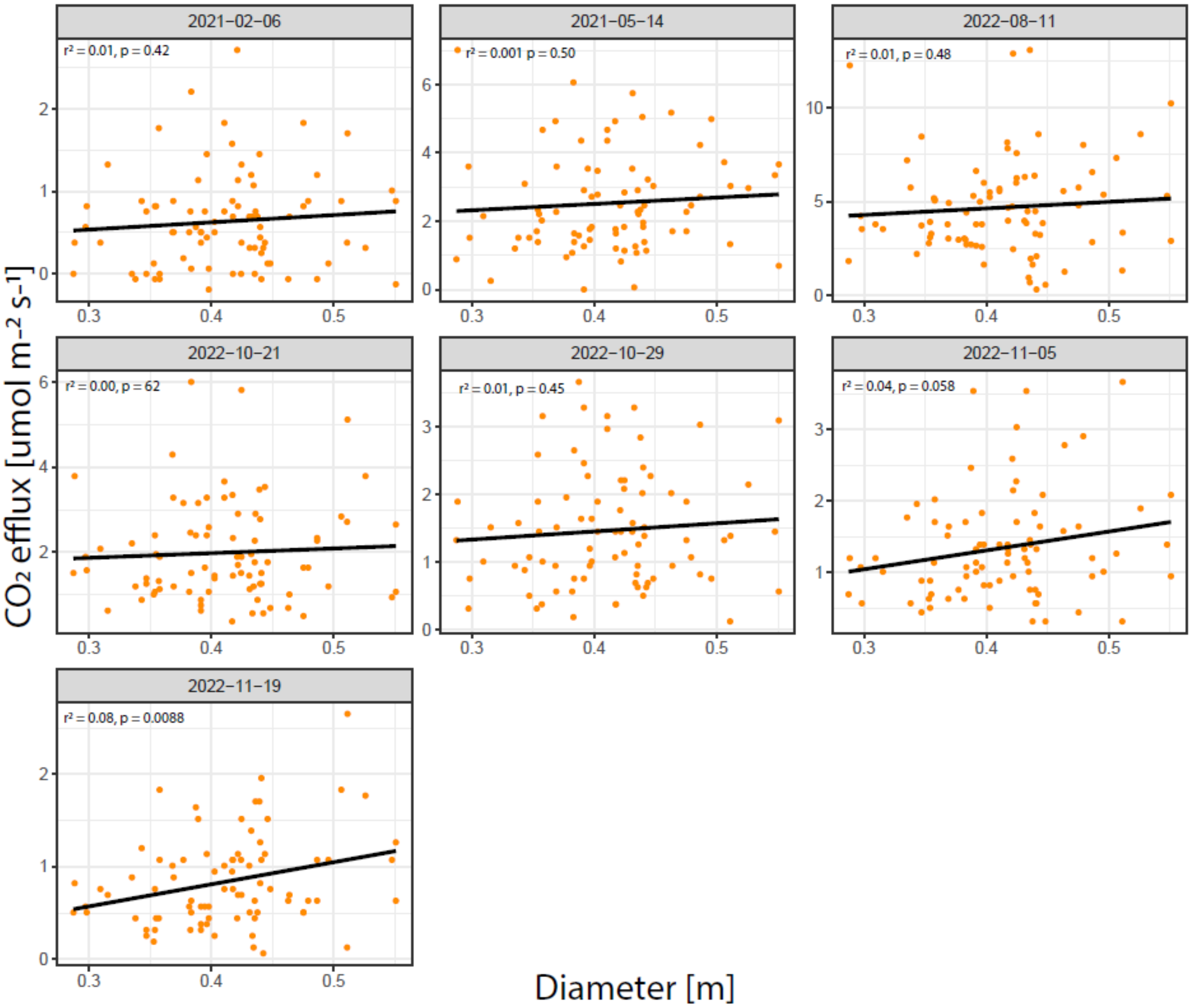

Figure 3.19. Linear regressions by date between soil CO_2 efflux diameter of the closest tree. Significant ($p < 0.05$) positive relationship on 2022-11-05 $r^2 = 0.04$ and 2022-11-19 $r^2 = 0.08$.

The Pearson's correlation coefficient between CO_2 efflux, electrical conductivity, tree diameter, and proximity to the nearest tree is shown in Figure 3.20. I found a significant ($p < 0.05$) positive relationship on 2022-10-21 $r^2 = 0.05$, 2022-11-05 $r^2 = 0.11$, and 2022-11-19 $r^2 = 0.16$ for proximity to nearest tree and CO_2 efflux as shown before. Another significant positive relationship found on 2022-11-05 $r^2 = 0.04$ and 2022-11-19 $r^2 = 0.08$ between the tree diameter and CO_2 efflux. There was a significant positive relationship on 2022-10-21 $r^2 = 0.04$ and a significant negative relationship on 2022-29-10 $r^2 = 0.05$ between electrical conductivity at 3 m depth and CO_2 efflux. Lastly, there was a significant positive relationship on 2022-10-21 $r^2 =$ 0.07 at 6 m depth between electrical conductivity and CO_2 efflux. The CO_2 efflux values showed a moderate level of correlation among themselves, which increased as the proximity of dates increased, although this correlation was not necessarily strong.

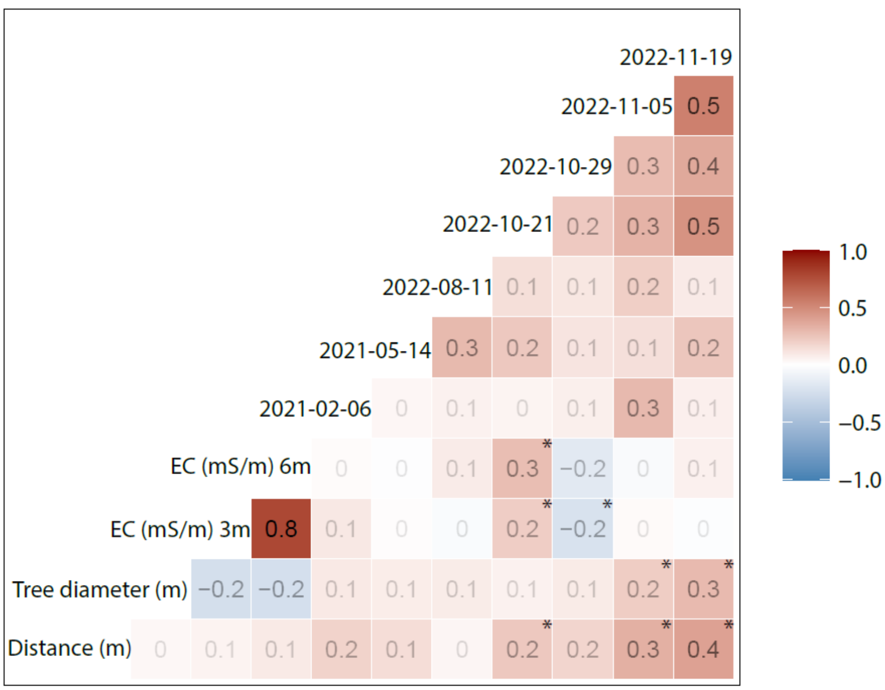

Figure 3.20. Heat map of Pearson's correlation coefficient between CO_2 efflux vs. distance from measuring point to closest tree, CO_2 efflux vs. closest tree diameter and CO_2 efflux vs. electrical conductivity among 7 measurement dates. Significant ($p < 0.05$) values are marked (*).

DISCUSSION

4.1 Spatial patterns and spatiotemporal CO_2 efflux from stationary and portable chambers

The soil CO_2 efflux did not show obvious spatial patterning related to regions within the field at the flood-irrigated pecan orchard. In other words, the CO_2 release is relatively uniform across the field without any significant variations or differences that can be observed visually. For this reason, the patterns are harder to predict, and further data collection is needed to quantify these patterns. During our observation period, we noticed that CO_2 efflux values were relatively low before the start of the irrigation season in February, but with the highest spatial variability (CV 90.9%). One explanation could be that during this dry and cold period, the high soil moisture content was limited to a very few areas, resulting in high variability in CO_2 efflux. As the irrigation season progressed, the CO_2 efflux values gradually increased and reached their peak in August with the least spatial variability (CV 55.4%). The CO_2 efflux values began to decrease afterward as we entered the fall and winter post-irrigation season. However, the spatial variability remained relatively constant (CVs 57.7-58.6%) compared to the variability during May-August (CVs 57.5-55.4%).

A similar study conducted on a semiarid agricultural land also found that the least spatial variability occurred during the growing season, while more variability was observed during the dry season (Oyonarte et al., 2012). They attributed this variation to transport processes in the soil during the dry period and to organic carbon and plant cover during the growing period. Although the irrigation schedule and growing season in their study differs from ours, the spatial variability pattern showed similarity to our study. In another study conducted on an agricultural dryland in China, it was found that irrigation highly influenced soil respiration (Yu et al., 2015). The CO_2

efflux values decreased significantly following irrigation when the soil water content exceeded the soil water field capacity. As the soil gradually dried out, the CO_2 efflux returned to normal levels. When combined with our own findings, these results emphasize the significant impact of irrigation that causes increases and decreases in CO_2 efflux not just spatially but also temporally.

The CO_2 efflux pattern at the Jornada shrubland site was more evident prior to the saturation experiment, likely due to the longer sampling time required compared to other dates. This resulted in higher efflux values during the morning and lower values during the afternoon, emphasizing the significance of measuring CO_2 efflux rates within a shorter timeframe to minimize the influence of daily temperature variations. These values were more consistent after the linear time correction. Following the saturation experiment, the CO_2 efflux rates of the points located within the irrigated plot showed a rapid and clearer increase. Besides water and temperature, the spatial CO_2 efflux patterns in drylands can be strongly influenced by the presence of rock fragments and biological soil crusts (Maestre, 2003; Maestre & Cortina, 2002). During the saturation experiment, a few points under the simulated rain plot showed a significant increase in CO_2 efflux compared to the rest of the points that were not under the irrigated plot and the variability was highest (CV 232%). The spatial variability at the natural site was much higher compared to the agricultural site at the pecan orchard (CV 232% vs. ~55%). Finally, in November, the CO_2 pattern was more consistent due to a shorter sampling period and had the least variability (CV 40.1%), but it had the highest CO_2 efflux values among the three sampling dates. Based on our observations of significantly high CO_2 fluxes after the saturation experiment, it aligns with existing literature on the topic. Specifically, previous research conducted on desert ecosystems has demonstrated that soil CO_2 efflux rates tend to notably rise after rainfall simulation events (Leon et al., 2014; Maestre & Cortina, 2003). The findings in our investigation of the creosote shrubland natural site illustrate the notable variability that can exist in CO_2 efflux in drylands (Schlesinger & Pilmanis, 1998).

My data showed that as the length of time from irrigation increased, effluxes decreased along with some of the spatial patterns and variability of CO_2 efflux. The strong relationship between soil CO_2 efflux, soil moisture and soil temperature has been highly studied (M. Almagro et al., 2009; Dilustro et al., 2005; Fang & Moncrieff, 2001; Maier et al., 2011; Tang et al., 2003). It is safe to imply for our study that in the summer months the temperature was very high (X. Liu et al., 2000) and the soils were very wet because of the ongoing flood irrigation at the pecan orchard, and that this is why we observed high efflux rates during that time. For our natural site at Jornada, the pattern was more noticeable at the beginning of the sampling time resulting from the higher CO_2 values in the morning. Overall, there was no other obvious spatial CO_2 efflux patterning related to regions within the field and further statistical analysis is needed to quantify it.

4.2 Spatial autocorrelation of soil CO_2 efflux

I found that CO_2 efflux values were generally well-correlated at small distances across most measurement dates (high partial sill values), but that this autocorrelation disappears quickly over distance (low range). The scale of autocorrelation for CO_2 efflux, as determined using the range from the variogram, decreased (range: 5-8 m) during the irrigation season compared to the dry down sequence after irrigation season (range: 14-15 m). I also found strong levels of spatial autocorrelation during the dry down sequence and less autocorrelation when the field was wetter and hotter. This may indicate that during times of high moisture and temperature, the water was more evenly distributed across the orchard, resulting in less variability in soil moisture levels and a lower degree of spatial autocorrelation. I found no spatial autocorrelation during one of the dry down sequence dates after irrigation season on 2022-10-29. Similarly to what we saw during this date, no spatial structure was observed for soil CO_2 efflux under drier conditions in a Canadian bare soil (Rochette et al., 1991). In contrast to this trend, researchers did not observe any spatial variability structure in a Brazilian bare soil field when the field was wetter (La Scala et al., 2000). They attributed this result to a rain event because of the increase in soil moisture, and soil temperature. However, their study was conducted on a shorter temporal scale. The lack of structure on the spatial variability model in October indicates that the CO_2 efflux values are independent of each other and random. This could happen if the CO_2 efflux is not affected by any spatial patterns or structures in the study area. As expected, the Jornada ranges were smaller (3-5 m) than those observed in the pecan orchard due to the smaller and denser vegetation. However, this difference in range size could also be a result of the smaller sampling scale employed in the study.

At the orchard, tree diameter had the largest geostatistical range (74 m) and the least variability (CV 12.7%) among my measured variables. Electrical conductivity had lower ranges (24-27 m) compared to the tree diameter and the variability was intermediate between the CO_2 efflux and tree diameter (CV 37-39%). These trends might be due to the larger sampling scale of the pecan trees or that the underlying patterns of electrical conductivity are more heterogeneous. In October, we observed significant positive and negative correlations between soil CO_2 efflux and electrical conductivity. Generally, there is a negative relationship between soil respiration and salinity in arid climates because saline soils can naturally absorb carbon dioxide via carbonate dissolution (Lai et al., 2012; Xie et al., 2009). The study area being a dryland agricultural region with naturally saline soils, combined with increased soil moisture from flood irrigation and runoff, may enhance the dissolution of pedogenic carbonates in the soil (Cox et al., 2018). Apart from this, other biological processes can affect the relationship between electrical conductivity and soil CO_2 efflux. For instance, when soil salinity is high, the microbial biomass decreases, becomes more stressed and is less metabolically efficient (Rietz & Haynes, 2003; Yan & Marschner, 2012). Overall, I conclude that the relationship between soil respiration and electrical conductivity is context-dependent and cannot be generalized without considering the specific conditions of the soil in question.

4.3 Spatiotemporal soil CO_2 efflux from stationary and portable chambers

We measured spatial and temporal soil CO_2 efflux rates for two sampling dates to compare the daily variability. We observed that while there is some degree of correlation between day-to-day variations and the consistency across different locations, the spatial patterns do exhibit a certain degree of variability, suggesting that a single day's measurements may not accurately represent the overall spatial pattern conditions. During the sampling period in the pecan orchard field, we noticed minimal temporal variation, while the differences in CO_2 efflux rates using the EGM-5 demonstrated the spatial variability across the field. This comparison increased confidence in our spatial measurements at the pecan orchard. However, for the Jornada site, we observed a more noticeable trend, where higher CO_2 fluxes occurred during the day and decreased in the afternoon. The steadier fluxes observed throughout the day at the pecan orchard may also be attributed to the shading effect of the trees. There is a strong correlation between tree canopy temperature and air and surface temperature (Berry et al., 2013; Cheung et al., 2021). It is widely recognized that temperature and soil respiration are closely related, as demonstrated by previous studies (M. Almagro et al., 2009; Dilustro et al., 2005; Fang & Moncrieff, 2001; Maier et al., 2011; Tang et al., 2003). The smaller local vegetation at the Jornada's natural desert setting compared to the pecan trees, resulting in higher surface temperatures and which in turn may cause a more significant temporal fluctuation in CO_2 levels.

4.4 Associations between soil CO_2 efflux and critical zone features

My findings revealed that the proximity to the closest tree and the size of the nearest tree can be at least a weak predictor of soil CO_2 efflux and can potentially explain some of its spatial patterns. Moreover, the tree diameter and proximity to the nearest tree are slightly better than electrical conductivity at explaining the variation within the spatial structure of soil CO_2 efflux. They provide some insight into the spatial structure; however, the relationship is weak. There is a lot of unexplained variation and there are other unmeasured factors that are contributing to the patterns seen in soil CO_2 efflux. These results align with previous studies that indicate a positive correlation between tree size and soil CO_2 efflux, suggesting that larger trees may generate higher levels of soil CO_2 efflux (Cavaleri et al., 2006; Schurman & Thomas, 2021). One possible explanation of this relationship is that larger trees with higher root extent might still have access to deep soil moisture (Burgess et al., 1998). This phenomenon also called 'hydraulic lift' (Richards & Caldwell, 1987), is the process by which plants transfer water from deep soil layers to drier soil layers through the root system. Because we observed a positive correlation between soil CO_2 efflux and larger trees towards the end of the irrigation season, the 'hydraulic lift' might have been a response to alleviate water stress for shallow-rooted plants during dry periods (Zegada-Lizarazu & Iijima, 2004). While we may find positive correlation between soil CO_2 efflux and tree size, the relationship between these variables is weak, and thus other factors such as soil moisture content, the drying conditions that could affect the magnitude of decomposition, and microbial activity are likely also at play.

I found that CO_2 efflux *increased* farther away from the trees after the irrigation season ended. Conversely, the measured efflux in forest ecosystems are often greater in proximity to a tree compared to locations at a short distance away (Butnor et al., 2006; Wiseman & Seiler, 2004). The authors of that study attributed this spatial difference in soil CO_2 efflux to variations in root biomass. Our results could be associated with lateral movement of respired CO_2 and could explain why we don't see higher CO_2 near the trees (Gough & Seiler, 2004; Pangle & Seiler, 2002) . The lateral movement of respired CO_2 is affected by soil texture and porosity (Le Dantec et al., 1999; Vodnik et al., 2006), implying that during the post irrigation season the soil was drier and probably had less clay content, thus facilitating the lateral diffusion of the soil CO_2. Another possible explanation could be that soil conditions can vary significantly between the areas underneath trees and those located away from tree canopies. This is because trees can have a significant impact on the soil and the ecosystem around them. Canopy cover affects soil respiration by regulating soil microclimate through changes in temperature and moisture, thus inducing changes in the spatial heterogeneity of soil respiration (Y. Liu et al., 2014; McCarthy & Brown, 2006). The presence of tree canopies can also affect the amount of sunlight that reaches the soil. Areas under tree canopies receive less direct sunlight than those located away from trees. This can result in cooler soil temperatures and slower rates of decomposition (Cortez, 1998), and can potentially explain why our results show higher soil CO_2 rates farther away from the trees compared to those that are closest to the tree.

My results suggest that there is only a weak correlation between soil CO_2 efflux, tree size, and proximity to the nearest tree. Thus, there are other factors that are likely determining the soil CO_2 efflux rates. Some of these factors could be root distribution (Vargas & Allen, 2008), root density (Janssens et al., 1998), vegetation type (Maestre & Cortina, 2003), soil texture (Cable et al., 2011), inter-canopy spaces (Gafford et al., 2011), soil organic matter fractions (María Almagro & Querejeta, 2013), higher root biomass and leaf area index (Leon et al., 2014). Although many of these factors were not measured during this work, especially partitioned root respiration and root biomass, the distance to the closest tree and the size of the tree can give us an idea of the potential root location and the respired CO_2 movement belowground. Further research is necessary to fully understand the complex interactions between CO_2 efflux, tree diameter and proximity to nearest tree and their effects on soil carbon cycling in agricultural drylands.

CONCLUSION

My results revealed that there was some spatial variability in CO_2 efflux explained by the tree size and proximity to nearest tree on the flood-irrigated pecan orchard. This relationship was slightly stronger compared to the correlation with electrical conductivity. I observed a clear and rapid efflux response to water addition at the creosote bush shrubland. Moreover, the CO_2 efflux also exhibited a more explicit diurnal variation than the pecan orchard, with higher values in the morning and lower values in the afternoon. However, further data collection is required to accurately quantify the spatial patterns in soil CO_2 efflux. I also found that there was strong spatial autocorrelation for soil CO_2 efflux at the flood-irrigated pecan orchard during the dry down sequence after the irrigation season, while less autocorrelation was observed when the field was the wettest and hottest. The findings of my study indicate a strong correlation between CO_2 efflux at short distances, followed by electrical conductivity at larger distances, and tree diameter at the greatest distance. While here I examined some of the possible drivers of spatial variability in soil CO_2 efflux, there are other unmeasured factors that are contributing to the spatial structure of soil CO_2 efflux besides electrical conductivity, tree diameter, and proximity to nearest tree. This study highlights the complex interaction between spatial variation of vegetation and surface soil features on soil CO_2 efflux within semi-arid ecosystems and dryland agriculture.

REFERENCES

Ahlström, A., Raupach, M. R., Schurgers, G., Smith, B., Arneth, A., Jung, M., Reichstein, M., Canadell, J. G., Friedlingstein, P., Jain, A. K., Kato, E., Poulter, B., Sitch, S., Stocker, B. D., Viovy, N., Wang, Y. P., Wiltshire, A., Zaehle, S., & Zeng, N. (2015). The dominant role of semi-arid ecosystems in the trend and variability of the land CO2 sink. *Science*, *348*(6237). https://doi.org/10.1126/science.aaa1668

Almagro, M., López, J., Querejeta, J. I., & Martínez-Mena, M. (2009). Temperature dependence of soil CO2 efflux is strongly modulated by seasonal patterns of moisture availability in a Mediterranean ecosystem. *Soil Biology and Biochemistry*, *41*(3). https://doi.org/10.1016/j.soilbio.2008.12.021

Almagro, María, & Querejeta, J. I. (2013). *Links between vegetation patterns , soil C and N pools and respiration rate under three different land uses in a dry Mediterranean ecosystem*. 641–653. https://doi.org/10.1007/s11368-012-0643-5

Arguez, A., Durre, I., Applequist, S., Vose, R. S., Squires, M. F., Yin, X., Heim, J. R. R., & Owen, T. W. (2012). NOAA's 1981–2010 U.S. Climate Normals: An Overview. *Bull Amer Meteor Soc*, *93*, 1687–1697. http://journals.ametsoc.org/doi/abs/10.1175/BAMS-D-11-00197.1

Bergametti, G., & Gillette, D. A. (2010). Aeolian sediment fluxes measured over various plant/soil complexes in the Chihuahuan desert. *Journal of Geophysical Research: Earth Surface*, *115*(3), 1–17. https://doi.org/10.1029/2009JF001543

Berry, R., Livesley, S. J., & Aye, L. (2013). Tree canopy shade impacts on solar irradiance received by building walls and their surface temperature. *Building and Environment, 69*. https://doi.org/10.1016/j.buildenv.2013.07.009

Biederman, J. A., Scott, R. L., Bell, T. W., Bowling, D. R., Dore, S., Garatuza-Payan, J., Kolb, T. E., Krishnan, P., Krofcheck, D. J., Litvak, M. E., Maurer, G. E., Meyers, T. P., Oechel, W. C., Papuga, S. A., Ponce-Campos, G. E., Rodriguez, J. C., Smith, W. K., Vargas, R., Watts, C. J., … Goulden, M. L. (2017). <scp>CO</scp> $_2$ exchange and evapotranspiration across dryland ecosystems of southwestern North America. *Global Change Biology*, *23*(10), 4204–4221. https://doi.org/10.1111/gcb.13686

Bohling, G. (2005). INTRODUCTION TO GEOSTATISTICS And VARIOGRAM ANALYSIS. In *Earth* (Issue October).

Buchmann, N. (2000). Biotic and abiotic factors controlling soil respiration rates in Picea abies stands. *Soil Biology and Biochemistry*, *32*(11–12), 1625–1635. https://doi.org/10.1016/S0038-0717(00)00077-8

Burgess, S. S. O., Adams, M. A., Turner, N. C., & Ong, C. K. (1998). The redistribution of soil water by tree root systems. *Oecologia*, *115*(3). https://doi.org/10.1007/s004420050521

Butnor, J. R., Johnsen, K. H., & Sanchez, F. G. (2006). Whole-tree and forest floor removal from a loblolly pine plantation have no effect on forest floor CO2 efflux 10 years after harvest. *Forest Ecology and Management*, *227*(1–2). https://doi.org/10.1016/j.foreco.2006.02.018

Cable, J. M., Ogle, K., Lucas, R. W., Huxman, T. E., Loik, M. E., Smith, S. D., Tissue, D. T., Ewers, B. E., Pendall, E., Welker, J. M., Charlet, T. N., Cleary, M., Griffith, A., Nowak, R. S., Rogers, M., Steltzer, H., Sullivan, P. F., & van Gestel, N. C. (2011). The temperature responses of soil respiration in deserts: A seven desert synthesis. *Biogeochemistry*, *103*(1), 71–90. https://doi.org/10.1007/s10533-010-9448-z

Carvalhais, N., Reichstein, M., Ciais, P., Collatz, G. J., Mahecha, M. D., Montagnani, L., Papale, D., Rambal, S., & Seixas, J. (2010). Identification of vegetation and soil carbon pools out of equilibrium in a process model via eddy covariance and biometric constraints. *Global Change Biology*, *16*(10). https://doi.org/10.1111/j.1365-2486.2010.02173.x

Cavaleri, M. A., Oberbauer, S. F., & Ryan, M. G. (2006). Wood CO2 efflux in a primary tropical rain forest. *Global Change Biology*, *12*(12). https://doi.org/10.1111/j.1365-2486.2006.01269.x

Cheung, P. K., Jim, C. Y., & Hung, P. L. (2021). Preliminary study on the temperature relationship at remotely-sensed tree canopy and below-canopy air and ground surface. *Building and Environment*, *204*. https://doi.org/10.1016/j.buildenv.2021.108169

Conant, R. T., Klopatek, J. M., & Klopatek, C. C. (2000). Environmental Factors Controlling Soil Respiration in Three Semiarid Ecosystems. *Soil Science Society of America Journal*, *64*(1), 383–390. https://doi.org/10.2136/sssaj2000.641383x

Cortez, J. (1998). Field decomposition of leaf litters: Relationships between decomposition rates and soil moisture, soil temperature and earthworm activity. *Soil Biology and Biochemistry*, *30*(6). https://doi.org/10.1016/S0038-0717(97)00163-6

Cox, C., Jin, L., Ganjegunte, G., Borrok, D., Lougheed, V., & Ma, L. (2018). Soil quality changes due to flood irrigation in agricultural fields along the Rio Grande in western Texas. *Applied Geochemistry*, *90*. https://doi.org/10.1016/j.apgeochem.2017.12.019

Cressie, N. (1990). The origins of kriging. *Mathematical Geology*, *22*(3). https://doi.org/10.1007/BF00889887

Darrouzet-Nardi, A. (2010). Landscape heterogeneity of differently aged soil organic matter constituents at the forest-Alpine Tundra Ecotone, Niwot Ridge, Colorado, U.S.A. *Arctic, Antarctic, and Alpine Research*, *42*(2), 179–187. https://doi.org/10.1657/1938-4246-42.2.179

Darrouzet-Nardi, A., Asaff, I.S., Mauritz, M., Roman, K., Keats, E., Tweedie, C.E., McLaren, J.R. (2023). Consistent microbial and nutrient resource island patterns during monsoon rain in a Chihuahuan Desert bajada shrubland. Ecosphere 14, e4475.

Darrouzet-Nardi, A., & Bowman, W. D. (2011). Hot Spots of Inorganic Nitrogen Availability in an Alpine-Subalpine Ecosystem, Colorado Front Range. *Ecosystems*, *14*(5), 848–863. https://doi.org/10.1007/s10021-011-9450-x

Darrouzet-Nardi, A., Reed, S. C., Grote, E. E., & Belnap, J. (2015). Observations of net soil exchange of CO2 in a dryland show experimental warming increases carbon losses in biocrust soils. *Biogeochemistry*, *126*(3), 363–378. https://doi.org/10.1007/s10533-015-0163-7

Dilustro, J. J., Collins, B., Duncan, L., & Crawford, C. (2005). Moisture and soil texture effects on soil CO2 efflux components in southeastern mixed pine forests. *Forest Ecology and Management*, *204*(1). https://doi.org/10.1016/j.foreco.2004.09.001

Entry, J. A., Sojka, R. E., & Shewmaker, G. E. (2004). Irrigation increases inorganic carbon in agricultural soils. *Environmental Management*, *33*(SUPPL. 1). https://doi.org/10.1007/s00267-003-9140-3

Fang, C., & Moncrieff, J. B. (2001). The dependence of soil CO2 efflux on temperature. *Soil Biology and Biochemistry*, *33*(2). https://doi.org/10.1016/S0038-0717(00)00125-5

Gafford, G. A. B., Scott, R. L., Jenerette, G. D., & Huxman, T. E. (2011). *The relative controls of temperature , soil moisture , and plant functional group on soil CO 2 efflux at diel , seasonal , and annual scales*. *116*, 1–16. https://doi.org/10.1029/2010JG001442

Ganjegunte, G. K., Clark, J. A., Parajulee, M. N., Enciso, J., & Kumar, S. (2018). Salinity Management in Pima Cotton Fields Using Sulfur Burner. *Agrosystems, Geosciences and*

Environment, *1*(1), 1–10. https://doi.org/10.2134/age2018.04.0006

Giardino, J. R., & Houser, C. (2015). Introduction to the Critical Zone. In *Developments in Earth Surface Processes* (Vol. 19). https://doi.org/10.1016/B978-0-444-63369-9.00001-X

Gibbens, R. P., McNeely, R. P., Havstad, K. M., Beck, R. F., & Nolen, B. (2005). Vegetation changes in the Jornada Basin from 1858 to 1998. *Journal of Arid Environments*, *61*(4), 651–668. https://doi.org/10.1016/j.jaridenv.2004.10.001

Gibbens, Robert P., & Lenz, J. M. (2001). Root systems of some Chihuahuan Desert plants. *Journal of Arid Environments*, *49*(2), 221–263. https://doi.org/10.1006/jare.2000.0784

Gough, C. M., & Seiler, J. R. (2004). The influence of environmental, soil carbon, root, and stand characteristics on soil CO2 efflux in loblolly pine (Pinus taeda L.) plantations located on the South Carolina Coastal Plain. *Forest Ecology and Management*, *191*(1–3). https://doi.org/10.1016/j.foreco.2004.01.011

Hanson, P. J., Edwards, N. T., Garten, C. T., & Andrews, J. A. (2000). *Separating root and soil microbial contributions to soil respiration : A review of methods and observations*. *C*, 115–146.

Havstad, K. M., Kustas, W. P., Rango, A., Ritchie, J. C., & Schmugge, T. J. (2000). Jornada Experimental Range: A unique arid land location for experiments to validate satellite systems. *Remote Sensing of Environment*, *74*(1), 13–25. https://doi.org/10.1016/S0034-4257(00)00118-8

Herbst, M., Bornemann, L., Graf, A., Welp, G., Vereecken, H., & Amelung, W. (2012). A geostatistical approach to the field-scale pattern of heterotrophic soil CO2 emission using covariates. *Biogeochemistry*, *111*(1–3), 377–392. https://doi.org/10.1007/s10533-011-9661-4

Hutyra, L. (2014). Terrestrial Ecosystems & the Carbon Cycle. *Global Change Biol.*, *1*(December 1994), 77–91.

Janssens, I. A., Barigah, S. T., & Ceulemans, R. (1998). Soil CO2 efflux rates in different tropical vegetation types in French Guiana. *Annales Des Sciences Forestieres*, *55*(6). https://doi.org/10.1051/forest:19980603

La Scala, N., Marques, J., Pereira, G. T., & Cora, J. E. (2000). Short-term temporal changes in the spatial variability model of CO2 emissions from a Brazilian bare soil. *Soil Biology and Biochemistry*, *32*(10), 1459–1462. https://doi.org/10.1016/S0038-0717(00)00051-1

Lai, L., Zhao, X., Jiang, L., Wang, Y., Luo, L., Zheng, Y., Chen, X., & Rimmington, G. M. (2012). Soil Respiration in Different Agricultural and Natural Ecosystems in an Arid Region. *PLoS ONE*, *7*(10), 2–10. https://doi.org/10.1371/journal.pone.0048011

Lal, R., & Kimble, J. M. (2000). Pedogenic carbonates and the global carbon cycle. In *Global Climate Change and Pedogenic Carbonates*.

Le Dantec, V., Epron, D., & Dufrêne, E. (1999). Soil CO2 efflux in a beech forest: Comparison of two closed dynamic systems. *Plant and Soil, 214*(1–2).

Leon, E., Vargas, R., Bullock, S., Lopez, E., Panosso, A. R., & La Scala, N. (2014). Hot spots, hot moments, and spatio-temporal controls on soil CO2 efflux in a water-limited ecosystem. *Soil Biology and Biochemistry*, *77*(June), 12–21. https://doi.org/10.1016/j.soilbio.2014.05.029

Liu, X., Lindemann, W. C., Whitford, W. G., & Steiner, R. L. (2000). Microbial diversity anti activity of disturbed soil in the northern chihuahuan desert. *Biology and Fertility of Soils*, *32*(3). https://doi.org/10.1007/s003740000242

Liu, Y., Liu, S., Wang, J., Zhu, X., Zhang, Y., & Liu, X. (2014). Variation in soil respiration under the tree canopy in a temperate mixed forest, central China, under different soil water conditions. *Ecological Research*, *29*(2). https://doi.org/10.1007/s11284-013-1110-5

Longenecker, D. E., Thaxton, E. L., & Lyerly, P. J. (1963). Cotton Production in Far West Texas with Emphasis on Irrigation and Fertilization. Texas FARMER Collection.

Luo, Y., Gerten, D., Le Maire, G., Parton, W. J., Weng, E., Zhou, X., Keough, C., Beier, C., Ciais, P., Cramer, W., Dukes, J. S., Emmett, B., Hanson, P. J., Knapp, A., Linder, S., Nepstad, D., & Rustad, L. (2008). Modeled interactive effects of precipitation, temperature, and [CO2] on ecosystem carbon and water dynamics in different climatic zones. *Global Change Biology*, *14*(9). https://doi.org/10.1111/j.1365-2486.2008.01629.x

Maestre, F. T. (2003). Small-scale spatial patterns of two soil lichens in semi-arid Mediterranean steppe. *Lichenologist*, *35*(1). https://doi.org/10.1006/lich.2002.0425

Maestre, F. T., & Cortina, J. (2002). Spatial patterns of surface soil properties and vegetation in a Mediterranean semi-arid steppe. *Plant and Soil*, *241*(2). https://doi.org/10.1023/A:1016172308462

Maestre, F. T., & Cortina, J. (2003). Small-scale spatial variation in soil CO2 efflux in a Mediterranean semiarid steppe. *Applied Soil Ecology*, *23*(3), 199–209. https://doi.org/10.1016/S0929-1393(03)00050-7

Maier, M., Schack-Kirchner, H., Hildebrand, E. E., & Schindler, D. (2011). Soil CO2 efflux vs. soil respiration: Implications for flux models. *Agricultural and Forest Meteorology*, *151*(12). https://doi.org/10.1016/j.agrformet.2011.07.006

McCarthy, D. R., & Brown, K. J. (2006). Soil respiration responses to topography, canopy cover, and prescribed burning in an oak-hickory forest in southeastern Ohio. *Forest Ecology and Management*, *237*(1–3). https://doi.org/10.1016/j.foreco.2006.09.030

McClaran, M. P. (1995). Desert grasslands and grasses. *The Desert Grassland*, 1–30.

Metz, E. M., Vardag, S. N., Basu, S., Jung, M., Ahrens, B., El-Madany, T., ... & Butz, A. (2023). Soil respiration–driven CO2 pulses dominate Australia's flux variability. Science, 379(6639), 1332-1335.

Norman, J. M., Kucharik, C. J., Gower, S. T., Baldocchi, D. D., Crill, P. M., Rayment, M., Savage, K., & Striegl, R. G. (1997). A comparison of six methods for measuring soil-surface carbon dioxide fluxes. *Journal of Geophysical Research Atmospheres*, *102*(24), 28771–28777. https://doi.org/10.1029/97jd01440

Ortiz, A. C., & Jin, L. (2021). Chemical and hydrological controls on salt accumulation in irrigated soils of southwestern U.S. *Geoderma*, *391*. https://doi.org/10.1016/j.geoderma.2021.114976

Ortiz, A. C., Jin, L., Ogrinc, N., Kaye, J., Krajnc, B., & Ma, L. (2022). Dryland irrigation increases accumulation rates of pedogenic carbonate and releases soil abiotic CO2. *Scientific Reports*, *12*(1). https://doi.org/10.1038/s41598-021-04226-3

Oyonarte, C., Rey, A., Raimundo, J., Miralles, I., & Escribano, P. (2012). The use of soil respiration as an ecological indicator in arid ecosystems of the SE of Spain: Spatial variability and controlling factors. *Ecological Indicators*, *14*(1). https://doi.org/10.1016/j.ecolind.2011.08.013

Pangle, R. E., & Seiler, J. (2002). Influence of seedling roots, environmental factors and soil characteristics on soil CO2 efflux rates in a 2-year-old loblolly pine (Pinus taeda L.) plantation in the Virginia Piedmont. *Environmental Pollution*, *116*. https://doi.org/10.1016/S0269-7491(01)00261-5

Panosso, A. R., Marques, J., Pereira, G. T., & La Scala, N. (2009). Spatial and temporal variability of soil CO 2 emission in a sugarcane area under green and slash-and-burn managements. *Soil and Tillage Research*, *105*(2), 275–282. https://doi.org/10.1016/j.still.2009.09.008

Parker, L. W., Miller, J., Steinberger, Y., & Whitford, W. G. (1983). Soil respiration in a chihuahuan desert rangeland. *Soil Biology and Biochemistry*, *15*(3). https://doi.org/10.1016/0038-0717(83)90075-5

Poulter, B., Frank, D., Ciais, P., Myneni, R. B., Andela, N., Bi, J., Broquet, G., Canadell, J. G., Chevallier, F., Liu, Y. Y., Running, S. W., Sitch, S., & Van Der Werf, G. R. (2014). Contribution of semi-arid ecosystems to interannual variability of the global carbon cycle. *Nature*, *509*(7502). https://doi.org/10.1038/nature13376

Prăvălie, R. (2016). Drylands extent and environmental issues. A global approach. In *Earth-Science Reviews* (Vol. 161, pp. 259–278). Elsevier B.V. https://doi.org/10.1016/j.earscirev.2016.08.003

Rayment, M. B., & Jarvis, P. G. (2000). Temporal and spatial variation of soil CO2 efflux in a Canadian boreal forest. *Soil Biology and Biochemistry*, *32*(1), 35–45. https://doi.org/10.1016/S0038-0717(99)00110-8

Richards, J. H., & Caldwell, M. M. (1987). Hydraulic lift: Substantial nocturnal water transport between soil layers by Artemisia tridentata roots. *Oecologia*, *73*(4). https://doi.org/10.1007/BF00379405

Rietz, D. N., & Haynes, R. J. (2003). Effects of irrigation-induced salinity and sodicity on soil microbial activity. *Soil Biology and Biochemistry*, *35*(6). https://doi.org/10.1016/S0038-0717(03)00125-1

Rochette, P., Desjardins, R. L., & Pattey, E. (1991). Spatial and temporal variability of soil respiration in agricultural fields. *Canadian Journal of Soil Science*, *71*(2). https://doi.org/10.4141/cjss91-018

Safriel, U., Adeel, Z., Niemeijer, D., Puigdefabregas, J., White, R., Lal, R., Winslow, M., Ziedler, J., Prince, S., Archer, E., King, C., Shapiro, B., Wessels, K., Nielsen, T., Portnov, B., Reshef, I., Thonell, J., Lachman, E., & Mcnab, D. (2005). Chapter 22: Dryland Systems. In *Ecosystems and Human Well-being: Current State and Trends, Volume 1*.

Sanderman, J. (2012). Can management induced changes in the carbonate system drive soil carbon sequestration? A review with particular focus on Australia. In *Agriculture, Ecosystems and Environment* (Vol. 155). https://doi.org/10.1016/j.agee.2012.04.015

Schlesinger, W. H., & Pilmanis, A. M. (1998). Plant-soil interactions in deserts. *Biogeochemistry*, *42*(1–2), 169–187. https://doi.org/10.1007/978-94-017-2691-7_9

Schlesinger, W. H., Raikks, J. A., Hartley, A. E., & Cross, A. F. (1996). On the spatial pattern of soil nutrients in desert ecosystems. *Ecology*, *77*(2). https://doi.org/10.2307/2265615

Schurman, J. S., & Thomas, S. C. (2021). Linking soil co2 efflux to individual trees: Size-dependent variation and the importance of the birch effect. *Soil Systems*, *5*(1). https://doi.org/10.3390/soilsystems5010007

Serna-Pérez, A., Monger, H. C., Herrick, J. E., & Murray, L. (2006). Carbon Dioxide Emissions from Exhumed Petrocalcic Horizons. *Soil Science Society of America Journal*, *70*(3), 795–805. https://doi.org/10.2136/sssaj2005.0099

Snyder, K. A., & Tartowski, S. L. (2006). Multi-scale temporal variation in water availability: Implications for vegetation dynamics in arid and semi-arid ecosystems. *Journal of Arid Environments*, *65*(2). https://doi.org/10.1016/j.jaridenv.2005.06.023

Stoyan, H., De-Polli, H., Böhm, S., Robertson, G. P., & Paul, E. A. (2000). Spatial heterogeneity of soil respiration and related properties at the plant scale. *Plant and Soil*, *222*(1–2), 203–214. https://doi.org/10.1023/a:1004757405147

Tamir, G., Shenker, M., Heller, H., Bloom, P. R., Fine, P., & Bar-Tal, A. (2011). Can Soil Carbonate Dissolution Lead to Overestimation of Soil Respiration? *Soil Science Society of America Journal*, *75*(4). https://doi.org/10.2136/sssaj2010.0396

Tan, W. F., Zhang, R., Cao, H., Huang, C. Q., Yang, Q. K., Wang, M. kuang, & Koopal, L. K. (2014). Soil inorganic carbon stock under different soil types and land uses on the Loess Plateau region of China. *Catena*, *121*, 22–30. https://doi.org/10.1016/j.catena.2014.04.014

Tang, J., Baldocchi, D. D., Qi, Y., & Xu, L. (2003). Assessing soil CO2 efflux using continuous measurements of CO2 profiles in soils with small solid-state sensors. *Agricultural and Forest Meteorology*, *118*(3–4). https://doi.org/10.1016/S0168-1923(03)00112-6

Valley, E. P. (n.d.). *Surnrnarv*.

Vargas, R., & Allen, M. F. (2008). Environmental controls and the influence of vegetation type, fine roots and rhizomorphs on diel and seasonal variation in soil respiration. *New Phytologist*, *179*(2), 460–471. https://doi.org/10.1111/j.1469-8137.2008.02481.x

Vodnik, D., Kastelec, D., Pfanz, H., Maček, I., & Turk, B. (2006). Small-scale spatial variation in soil CO2 concentration in a natural carbon dioxide spring and some related plant responses. *Geoderma*, *133*(3–4). https://doi.org/10.1016/j.geoderma.2005.07.016

Wiseman, P. E., & Seiler, J. R. (2004). Soil CO2 efflux across four age classes of plantation loblolly pine (Pinus taeda L.) on the Virginia Piedmont. *Forest Ecology and Management*, *192*(2–3). https://doi.org/10.1016/j.foreco.2004.01.017

Wu, H., Guo, Z., Gao, Q., & Peng, C. (2009). Distribution of soil inorganic carbon storage and its changes due to agricultural land use activity in China. *Agriculture, Ecosystems and*

Environment, *129*(4). https://doi.org/10.1016/j.agee.2008.10.020

Xie, J., Li, Y., Zhai, C., Li, C., & Lan, Z. (2009). CO2 absorption by alkaline soils and its implication to the global carbon cycle. *Environmental Geology*, *56*(5). https://doi.org/10.1007/s00254-008-1197-0

Yan, N., & Marschner, P. (2012). Response of microbial activity and biomass to increasing salinity depends on the final salinity, not the original salinity. *Soil Biology and Biochemistry*, *53*. https://doi.org/10.1016/j.soilbio.2012.04.028

Yu, Y., Zhao, C., Zhao, Z., Yu, B., & Zhou, T. (2015). Soil respiration and the contribution of root respiration of cotton (Gossypium hirsutum L.) in arid region. *Acta Ecologica Sinica*, *35*(3). https://doi.org/10.1016/j.chnaes.2015.04.001

Zegada-Lizarazu, W., & Iijima, M. (2004). Hydrogen stable isotope analysis of water acquisition ability of deep roots and hydraulic lift in sixteen food crop species. *Plant Production Science*, *7*(4). https://doi.org/10.1626/pps.7.427

VITA

Viridiana Orona earned her Bachelor of Science in Environmental Science from The University of Texas at El Paso in 2017. During her undergraduate studies, she conducted aquatic ecology research alongside Dr. Vanessa Lougheed and presented her findings at the Society of Wetland Scientist annual meeting. Following graduation, Orona joined Adastra Ecological Services Inc. in El Paso, Texas, as an environmental consultant.

In fall of 2019, Orona was admitted to the master's program in Environmental Science at The University of Texas at El Paso, which is under the Department of Earth, Environmental and Resource Sciences. She pursued her studies under the guidance of Dr. Anthony Darrouzet-Nardi, with a focus on dryland carbon fluxes. While pursuing her graduate degree, Orona worked as a biological science technician GS-05 at Saguaro National Park, a position she held for a year. As part of her graduate studies, Orona conducted research on the spatial variability in soil CO_2 fluxes in the Chihuahuan desert, using geostatistical techniques. This research served as the basis for her thesis.

Email: viridiana.orona@gmail.com

This thesis was typed by Viridiana Orona.